

Performance of the ATLAS Level-1 topological trigger in Run 2

ATLAS Collaboration; Newman, Paul

DOI:

[10.1140/epjc/s10052-021-09807-0](https://doi.org/10.1140/epjc/s10052-021-09807-0)

License:

Creative Commons: Attribution (CC BY)

Document Version

Publisher's PDF, also known as Version of record

Citation for published version (Harvard):

ATLAS Collaboration & Newman, P 2022, 'Performance of the ATLAS Level-1 topological trigger in Run 2', *European Physical Journal C*, vol. 82, no. 1, 7. <https://doi.org/10.1140/epjc/s10052-021-09807-0>

[Link to publication on Research at Birmingham portal](#)

General rights

Unless a licence is specified above, all rights (including copyright and moral rights) in this document are retained by the authors and/or the copyright holders. The express permission of the copyright holder must be obtained for any use of this material other than for purposes permitted by law.

- Users may freely distribute the URL that is used to identify this publication.
- Users may download and/or print one copy of the publication from the University of Birmingham research portal for the purpose of private study or non-commercial research.
- User may use extracts from the document in line with the concept of 'fair dealing' under the Copyright, Designs and Patents Act 1988 (?)
- Users may not further distribute the material nor use it for the purposes of commercial gain.

Where a licence is displayed above, please note the terms and conditions of the licence govern your use of this document.

When citing, please reference the published version.

Take down policy

While the University of Birmingham exercises care and attention in making items available there are rare occasions when an item has been uploaded in error or has been deemed to be commercially or otherwise sensitive.

If you believe that this is the case for this document, please contact UBIRA@lists.bham.ac.uk providing details and we will remove access to the work immediately and investigate.



Performance of the ATLAS Level-1 topological trigger in Run 2

ATLAS Collaboration*

CERN, 1211 Geneva 23, Switzerland

Received: 5 May 2021 / Accepted: 4 November 2021 / Published online: 5 January 2022
© CERN for the benefit of the ATLAS collaboration 2021

Abstract During LHC Run 2 (2015–2018) the ATLAS Level-1 topological trigger allowed efficient data-taking by the ATLAS experiment at luminosities up to $2.1 \times 10^{34} \text{ cm}^{-2} \text{ s}^{-1}$, which exceeds the design value by a factor of two. The system was installed in 2016 and operated in 2017 and 2018. It uses Field Programmable Gate Array processors to select interesting events by placing kinematic and angular requirements on electromagnetic clusters, jets, τ -leptons, muons and the missing transverse energy. It allowed to significantly improve the background event rejection and signal event acceptance, in particular for Higgs and B -physics processes.

Contents

1 Introduction	1
2 The ATLAS detector and trigger architecture	1
3 The L1 topological processor	2
4 The topological algorithms	5
5 Simulation and validation	5
6 Trigger performance	7
6.1 B -physics	7
6.2 Higgs physics	7
6.3 Long-lived particles	9
6.4 Large- R jets	9
7 Conclusions	10
References	12

1 Introduction

During Run 2, the Large Hadron Collider (LHC) delivered proton–proton (pp) collisions to the ATLAS experiment [1] with instantaneous luminosities up to $2.1 \times 10^{34} \text{ cm}^{-2} \text{ s}^{-1}$ and a centre-of-mass energy of 13 TeV. The very high instantaneous luminosity, accompanied by unprecedented rates of simultaneous pp interactions (pile-up) per bunch crossing

(BC), placed stringent operational constraints [2] on the ATLAS trigger system [3] to efficiently select the collision events relevant for the ATLAS physics programme. Events from the 40 MHz BCs were accepted at a reduced rate compatible with the detector readout, storage and offline computing resources, about 1–1.5 kHz on average.

The Level-1 (L1) trigger is the first rate-reducing step in the ATLAS trigger system. As shown in Fig. 1, the rate of events selected by some L1 physics triggers, named trigger ‘items’ in this paper, increases with the LHC instantaneous luminosity. To cope with such a rate increase, three approaches were used previously: tightening the requirements on the selected trigger objects, with a potential loss in signal acceptance; recording only one event in every N events (trigger prescale), with a consequent loss of integrated luminosity; or combining different trigger objects.

All three approaches cause some loss of interesting data, and this is particularly unfavourable for physics signatures having low-momentum final-state particles. For the first time in ATLAS, the L1 topological trigger (L1Topo) provided the ability to implement topological requirements, i.e. criteria based on the kinematic relations between objects, to improve the rejection of background events while preserving high acceptance for signal events.

This paper describes the performance of the L1Topo trigger system during the data-taking in 2017 and 2018. The paper is organised as follows. The ATLAS detector and the architecture of the trigger system are described in Sect. 2. An overview of the topological processor and its algorithms is presented in Sects. 3 and 4. The results of the validation procedure for such algorithms and their performance in physics events are discussed in Sects. 5 and 6, followed by the conclusions in Sect. 7.

2 The ATLAS detector and trigger architecture

The ATLAS experiment [1] at the LHC is a multipurpose particle detector with a forward–backward symmetric cylin-

* e-mail: atlas.publications@cern.ch

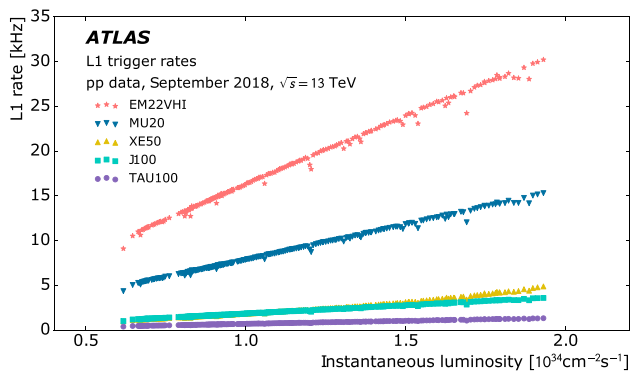


Fig. 1 Event rate of selected L1 trigger items as a function of the instantaneous luminosity in an LHC fill taken in September 2018 with a peak luminosity of $2.0 \times 10^{34} \text{ cm}^{-2} \text{ s}^{-1}$ and a peak average number of interactions per BC of 56. Presented are rates of some representative single-object trigger items that have not been prescaled. These trigger items are based on such objects as electromagnetic clusters (EM), muon candidates (MU), jet candidates (J), missing transverse energy (XE) and τ -lepton candidates (TAU). The number in the trigger name denotes the trigger transverse momentum threshold in GeV. The letters following the threshold value in the EM22VHI trigger refer to details of the selection: variable thresholds (V), hadronic isolation (H), and electromagnetic isolation (I)

dricl geometry and a near 4π coverage in solid angle.¹ It consists of an inner tracking detector surrounded by a thin superconducting solenoid providing a 2T axial magnetic field, electromagnetic and hadronic calorimeters, and a muon spectrometer. The inner tracking detector covers the pseudorapidity range $|\eta| < 2.5$. It consists of silicon pixel, silicon microstrip, and transition-radiation tracking detectors. Lead/liquid-argon sampling calorimeters provide electromagnetic energy measurements with high granularity for $|\eta| < 2.5$. A steel/scintillator-tile hadron calorimeter covers the central pseudorapidity range ($|\eta| < 1.7$). The end-cap and forward regions are instrumented with calorimeters based on liquid argon technology for both the electromagnetic (EM) and hadronic energy measurements up to $|\eta| = 4.9$. The muon spectrometer surrounds the calorimeters and is based on three large air-core toroidal superconducting magnets with eight coils each. The field integral of the toroids ranges between 2.0 and 6.0 Tm across most of the detector. The muon spectrometer includes three layers of high-precision tracking chambers which provide coverage in the range $|\eta| < 2.7$, and fast detectors for triggering in the range $|\eta| < 2.4$.

¹ ATLAS uses a right-handed coordinate system with its origin at the nominal interaction point (IP) in the centre of the detector and the z -axis along the beam pipe. The x -axis points from the IP to the centre of the LHC ring, and the y -axis points upwards. Cylindrical coordinates (r, ϕ) are used in the transverse plane, ϕ being the azimuthal angle around the z -axis. The pseudorapidity is defined in terms of the polar angle θ as $\eta = -\ln \tan(\theta/2)$.

The ATLAS experiment uses a two-level trigger system to select interesting events to record and analyse offline. The L1 trigger is hardware-based and uses a subset of the detector information to accept events from the 40 MHz LHC pp BCs at a rate below 100 kHz, which is the maximum detector readout rate. This is followed by a software-based high-level trigger (HLT) which reduces the event rate to around 1 kHz on average, constrained by a data storage capability of a few hundred MB/s [4].

The L1 trigger system, sketched in Fig. 2, consists of the calorimeter trigger (L1Calo) [5] and muon trigger (L1Muon) [6] systems, which compute the multiplicity of calorimeter energy clusters and muons above a transverse momentum (p_T) threshold (representing the minimum energy required),² as well as the Central Trigger Processor (CTP), which receives this information and computes the final L1 decision. In 2015 and 2016, new modules were installed in the real-time data path. The L1Calo and L1Muon systems were respectively upgraded with the Common Merger Modules (CMX) and the Muon Interface to L1Topo (MUCTPI2Topo) modules to store the momentum and angle (η and ϕ coordinate) information for each candidate object and propagate it to the new L1Topo processor. For the first time in ATLAS, this information was available in a single L1 trigger system and used to compute kinematic quantities and relations among multiple trigger objects, such as angular distances or invariant masses.

3 The L1 topological processor

The L1Topo system consists of a single processor crate equipped with two identical AdvancedTCA-compliant modules [7]. Pictures of one of the L1Topo modules before fibre assembly and of the full L1Topo system during operation are shown in Fig. 3. Each module has two processor Field Programmable Gate Arrays (FPGAs) (Xilinx Virtex7 [8]) to run the algorithms and one controller FPGA (Kintex7 [9]) responsible for the readout and all communication logic to interface to the external trigger systems.

A sketch of the architecture of the topological algorithms is shown in Fig. 4. The input data are sent via optical fibres at a speed of 6.4 Gb/s per line to the L1Topo system backplane and front-panel from the L1Calo and L1Muon systems, respectively. The data format is defined by Trigger Objects (TOBs), which are bit arrays encoding the position (η, ϕ),

² L1Calo triggers compute the multiplicity of clusters above transverse energy (E_T) thresholds, while L1Muon triggers compute the multiplicity of muons above transverse momentum (p_T) thresholds.

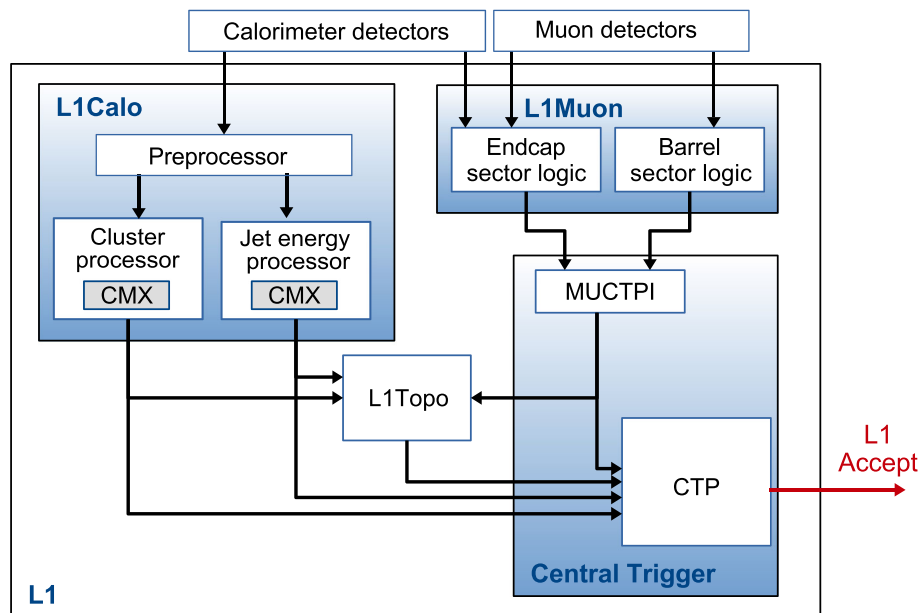


Fig. 2 The ATLAS L1 trigger system in Run 2 [2]

p_T , and further qualifying information³ for each object. The maximum numbers of different TOBs that can be received by the L1Topo system in one event are: 64 jet TOBs, 120 EM TOBs [10], 120 tau TOBs, 32 muon TOBs [6] and 1 missing transverse energy TOB [11]; the maximum number of TOBs received in the L1Topo system was found to be well within the constraints imposed by the physics cases of interest for the L1Topo trigger. As shown in Table 1, each type of TOB is characterised by a different granularity and bitwise precision for p_T and the $|\eta|$ and ϕ coordinates.

The optical signals are converted into electrical signals via Avago miniPODs [12] and then directed into the processor FPGAs, where they are deserialised in multi-gigabit transceivers. In each module, both processors are supplied with the same data, so that they can operate independently and in parallel. For each algorithm the resulting output action consists of setting two bits: the algorithm decision and the overflow bit. The overflow bit is set if any module of the L1Calo or L1Muon systems identifies more objects than it can provide to L1Topo: 5 (4) clusters (jets) per input L1Calo CMX module, or 2 muons per L1Muon Interface Octant board (MIOCT) [13], respectively. The logical OR of the two bits is then transmitted to the CTP for use in the L1 trigger decision.

Thanks to the extensive logic resources of the processor FPGAs, up to 128 topological algorithms (32 per processor FPGA) can be executed on the real-time data path and are configured using a set of parameters. By the end of 2018,

a total of 113 topological algorithms were implemented in VHDL [14], validated and operated. Lookup table operations dominate the resource usage in the FPGAs, as shown in Table 2 per FPGA together with the number of output bits.

The total latency of the L1Topo system is ~ 200 ns, corresponding to eight LHC BCs of 25 ns. As summarised in Fig. 5, 50 ns are used to receive and deserialise the data, 25 ns for their synchronisation and 75 ns are dedicated to the execution of the topological algorithms. The remaining 50 ns accounts for the data transmission through cables from the input source channels to L1Topo and from L1Topo to the final destination. Regarding the topological algorithms, the first 50 ns are used to filter the input TOBs in order to reduce the number of possible combinations when considering relations among objects, thus reducing the resource usage per algorithm. Technically, this is achieved by creating two types of filtered lists using the so-called ‘sort/select’ algorithms in Fig. 4. The first list type is created by sorting the TOBs by p_T and taking the first six leading objects. The second list type is created by selecting the first ten objects above a p_T threshold as ordered in the input source channel and received in the FPGA. An overflow bit is set for events with a second list type of more than ten TOBs. The length of these filtered lists is mostly limited by latency constraints, and it is adequate for most physics signatures. Finally, the remaining 25 ns in the algorithm execution are used to run the decision algorithms on the desired TOB lists. During Run 2 operations, a total of 17 lists including the two types were considered for the whole L1Topo system.

³ Examples are the isolation of electromagnetic clusters and τ -leptons, or the jet momentum obtained by clustering the object with a larger window size.

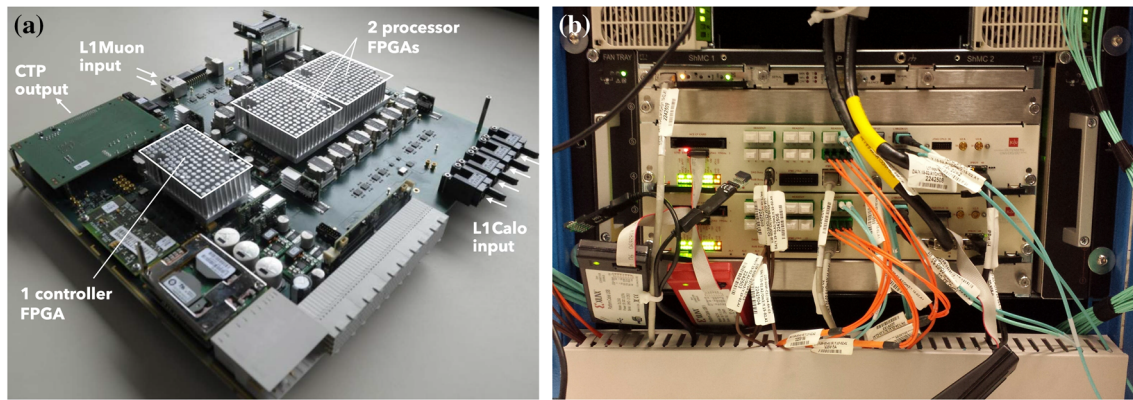


Fig. 3 a One of the L1Topo modules before fibre assembly, b the L1Topo system in operation

Fig. 4 Structure of the topological algorithms. The diagram provides a schematic view of the L1Topo data-flow, starting from the full TOBs input list to the output of the topological algorithms. Different kinds of input TOBs can be combined in each algorithm as needed for the physics signature. One LHC BC interval corresponds to 25 ns

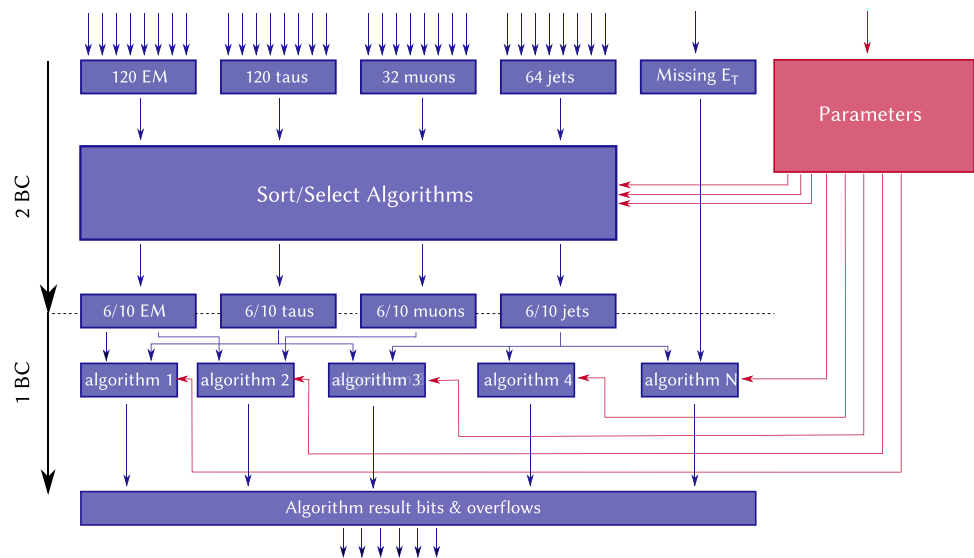


Table 1 Coordinate granularity and range for all the TOBs input to L1Topo. The $\eta \times \phi$ granularity for EM, tau and jet TOBs depends upon the detector system and readout; it ranges between 0.1×0.1 for EM and tau TOBs to 1.7×0.2 for jet TOBs with $|\eta| \geq 3.2$. The precision of the

bitwise representation of each TOB is also shown. The p_T measurement for muon TOBs used in L1Topo corresponds to the three available L1 p_T thresholds, and the η granularity is irregular ranging between 0.2 and 0.4

TOB type	Coordinate granularity			$ \eta $ range	Bitwise precision (number of bits)		
	p_T [GeV]	η	ϕ [rad]		p_T	η	ϕ
EM and tau	0.5	0.1	0.1	[0, 2.5]	8	6	6
	1	0.2	0.2		10	5	5
Jets	1	1.7	0.2	[3.2, 4.9]			
Muons	p_T [GeV] (thresholds)	η	ϕ [rad]	[0, 2.4]	p_T	η	ϕ
	{4, 6, 10}	0.2–0.4	0.1		2	6	6
E_T^{miss}	E_x [GeV]	E_y [GeV]	ϕ [rad]	-	E_x	E_y	ϕ
	1	1	0.1		16	16	6

Table 2 Resources used for lookup table blocks (Configurable Logic Blocks [8]) and number of output bits per processor FPGA out of a maximum of 32

Processor FPGA	1	2	3	4
Percentage of lookup table blocks utilised	50%	58%	71%	71%
Number of output bits	32	23	27	31

The set of criteria, the corresponding threshold values, and the lists of input objects are read from a programmable trigger menu [2] for each algorithm.

4 The topological algorithms

This section provides a general overview of the topological algorithms and their scope, while more details of specific use-cases are discussed in Sect. 6.

Different categories of topological algorithms have been implemented in L1Topo to address the needs of physics analyses and to help in the commissioning of new systems of the ATLAS detector. A complete list of topological algorithms is detailed in Table 3. The exact L1 trigger object input(s) to the algorithms, their specific requirements in terms of p_T , and the exact selection cuts applied by the algorithms are configurable and defined in the ATLAS trigger menu [16–18]. The trigger menu configuration can be changed during runtime, while the topological algorithms are defined in L1Topo firmware and cannot be modified during the data-taking without remotely accessing the L1Topo boards.

Examples of topological algorithms include angular requirements, invariant mass or transverse mass requirements, and global event requirements, with the flexibility to use central ($|\eta| < 3.2$ for jets, $|\eta| < 1.0$ for muons) and/or forward ($|\eta| > 3.2$ for jets, $|\eta| > 1.0$ for muons) L1 trigger objects. Calorimeter and muon information can also be combined, for example to search for lepton-flavour-violating $B_{(s)}^0 \rightarrow e^\pm \mu^\mp$ decays [19]. Also, L1 trigger objects can be required to come from different BCs, a requirement that can be useful in searching for heavy long-lived highly ionising particles that may be detected during the BC following the collision.

Angular selection criteria include requirements on the polar and azimuthal distances ($\Delta\eta$ and $\Delta\phi$) between two or

more trigger objects of the same or different type. These distances can be tailored to the kinematic properties of specific signal processes to select the objects satisfying the criteria or to discard a pair of overlapping objects from different lists. Algorithms summing the energy of all the objects inside a cone of a certain radius (referred to as simple cone algorithms) are also available and used to seed HLT triggers for large-radius jets. They have proven to be helpful in analyses exploiting jet substructure.

Topological mass and event criteria include invariant and transverse masses (m_{inv} and m_T), frequently used in many physics analyses, as well as event hardness (H_T), defined as the scalar p_T sum of all jet TOBs in the event.

Window acceptance selections place geometrical requirements on the azimuthal and pseudorapidity positions of given trigger objects. They are most useful in the commissioning of new systems or testing of prototypes by providing specific triggers limited only to their acceptance area, with only a marginal impact on the total ATLAS L1 budget rate. This has been used, for example, to study the hardware Fast Tracker [20] system partly installed during Run 2 and to commission the demonstrator set-up installed to verify the full functionality of the new Liquid Argon trigger readout system for the Phase-I upgrade [21].

5 Simulation and validation

The logic of the topological algorithms and their implementation in the hardware is validated at various levels, before and during data-taking. Before data-taking operations, the firmware is simulated in VHDL and basic checks of the internal logic consistency are performed. Well-defined input data are processed through the hardware via a playback mechanism and the decisions are examined. All L1Topo algorithms are also simulated and coded within the L1 and HLT software framework as well as stand-alone. This allows the validation and optimisation of the algorithms in terms of expected trigger rates and signal acceptances.

The L1Topo system and its integration with the other ATLAS systems is tested and validated in situ outside data-taking periods. In these tests, ‘hot towers’ are generated in the trigger system by overwriting the normal digitisation parameters of selected channels in the L1 calorimeter trigger elec-

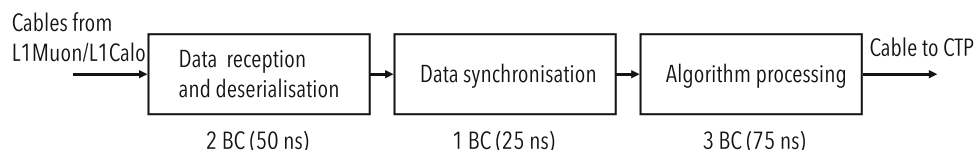


Fig. 5 Latency of the L1Topo system. The total latency is ~ 200 ns: 150 ns account for the operation of the system as shown in the figure, and the remaining 50 ns account for the length of the input and output cables

Table 3 List of topological algorithms implemented in Run 2. The input L1 trigger objects are required to pass configurable p_T threshold, η and isolation requirements. Trigonometric functions in the FPGAs are calculated using lookup tables

Algorithm	Definition
Pseudorapidity distance: $x_1 \leq \Delta\eta = \eta_1 - \eta_2 \leq x_2$	Pseudorapidity difference between the objects of two given input lists. The lower and upper bounds (x_1, x_2) are configurable parameters of the algorithm
Azimuthal distance: $y_1 \leq \Delta\phi = \phi_1 - \phi_2 \leq y_2$	Azimuthal distance between the objects of two given input lists. The lower and upper bounds (y_1, y_2) are configurable parameters of the algorithm
Box cuts: $x_1 \leq \Delta\eta \leq x_2$ and $y_1 \leq \Delta\phi \leq y_2$	Combination of $\Delta\eta$ and $\Delta\phi$ requirements with configurable lower and upper bounds (x_1, y_1, x_2, y_2). The same pair of objects must satisfy both conditions
Window cuts: $x_1 < \eta < x_2$ and $y_1 < \phi < y_2$	Requirement on the pseudorapidity and azimuthal positions of the objects given in an input list. The lower and upper bounds (x_1, y_1, x_2, y_2) are configurable parameters of the algorithm
Angular distance: $x_1^2 \leq \Delta R^2 = (\Delta\phi)^2 + (\Delta\eta)^2 \leq x_2^2$	Angular distance between the objects of two given input lists. The lower and upper bounds (x_1, x_2) are configurable parameters of the algorithm
Disambiguation: $\phi_1 \neq \phi_2$ OR $\eta_1 \neq \eta_2, \Delta R > x$	Takes two or three input lists and checks the spatial separation between each pair. For objects with the same granularity the ϕ and η coordinates are used directly, otherwise a requirement on ΔR is imposed
Ratio: $O_1 \geq x \cdot O_2$	Takes two input lists and for two objects in the same location ($\phi_1 = \phi_2$ AND $\eta_1 = \eta_2$) the ratio of two quantities is required to be above a threshold. The threshold (x) and the two quantities (O_1, O_2) are configurable parameters of the algorithm
Invariant mass: $x_1^2 \leq m_{\text{inv}}^2 = 2 E_{T,1} E_{T,2} (\cosh \Delta\eta - \cos \Delta\phi) \leq x_2^2$	Invariant mass of each pair of objects in two input lists. If the two input lists are different, the two objects used in the mass computation must satisfy the disambiguation criteria. The lower and upper bounds (x_1, x_2) are configurable parameters of the algorithm
Transverse mass: $x_1^2 \leq m_T^2 = 2 E_{T,1} E_T^{\text{miss}} (1 - \cos \Delta\phi) \leq x_2^2$	Transverse mass of the E_T^{miss} and the objects in one input list. The lower and upper bounds (x_1, x_2) are configurable parameters of the algorithm
Event hardness: $H_T > x$	Scalar sum of the transverse momenta of all or a selected number of jets. Additional requirements on the jet p_T or η are possible. The threshold (x) is a configurable parameter of the algorithm
Simple cone: $\sum_{\Delta R < 1.0} E_T^{\text{jet}} > x$	Sums the energy of jet TOBs with $E_T \geq 15$ GeV and centre within a cone of radius $\Delta R = 1.0$ around each jet [5, 15]; jets considered in the energy sum are distinct from the jet defining the cone centre. The threshold (x) for the energy sum is a parameter of the algorithm
Late muon	Finds the highest- p_T muon in the next BC and combines it with the input lists associated with the current BC. This results in a tighter latency budget for this algorithm

tronics with an alternative calibration that converts pedestal fluctuations, which would normally be removed by a noise cut, into a high- p_T signal. These are artificially formed in predefined regions of the subdetectors and issue a trigger that is used as input to the L1Topo hardware. By knowing the exact position of the regions where the trigger originated, L1Topo algorithms requiring a given angular position can be cross-checked. The time of the arrival of the decisions is also checked to ensure that they are all well aligned with the triggered events.

Once the firmware is validated and the L1Topo system well aligned in time, it is deployed for data-taking. During data-taking, the system is constantly monitored. All L1Topo algorithms are simulated in the HLT software running online in the HLT computing farm. A fraction of the L1 accepted events are processed in real time through this simulation at the HLT. This allows the comparison of the L1Topo hardware decisions and the simulated decisions both during and after data-taking. Both the statistical and event-by-event dif-

ferences are displayed in various histograms for online monitoring [2]. To achieve a precise comparison, the algorithms are simulated using integers instead of floating-point precision for the TOBs properties, as used in the L1Topo hardware. However, the exact implementation of the hardware logic in software is difficult to achieve and differences between simulation and hardware decisions at rates of a few per mille for less than 10% of the L1Topo algorithms were observed for the following reasons. Most topological algorithms use lists of TOBs ordered by decreasing p_T . In cases where the TOBs have identical p_T , there is ambiguity in the calculation of the kinematical variables that use them, such as invariant masses or differences in object position, potentially resulting in different trigger decisions. These ambiguities were fully simulated only for the case of muon TOBs. In addition, the hardware decisions take into account overflow conditions, which are not simulated. The rate of overflows during the pp data-taking was at most a few Hz.

6 Trigger performance

By offering a large variety of kinematic selections, the topological triggers can introduce requirements at L1 that are inspired by offline physics analyses. This approach results in significantly improved background event rejection and improved acceptance of physics signal events for many analyses, allowing the strict constraints of the L1 rate to be met, despite the increase in the instantaneous luminosity. This section highlights the performance of the topological triggers for a few chosen physics signatures.

6.1 B -physics

The first example is taken from the ATLAS B -physics programme, which strongly benefits from the use of L1Topo triggers. Many of these analyses are based on the identification of B and J/ψ mesons via their decay products, including very low p_T electron and muon pairs. For example, for the $J/\psi \rightarrow \mu\mu$ selection [22], the non-topological trigger requires two muons with p_T above 6 GeV. As shown in Fig. 6a, this trigger yields a L1 accept rate of up to 0.8 kHz for a luminosity of $\sim 1.9 \times 10^{33} \text{ cm}^{-2}\text{s}^{-1}$. However, by introducing topological requirements at trigger level that are closer to the actual selections in the offline analysis, such as requiring the angular separation between the two muon TOBs to be in the range $0.2 \leq \Delta R(\mu_1, \mu_2) \leq 1.5$ and the invariant mass of the dimuon pair ($m(\mu_1, \mu_2)$) to be in the range 2–9 GeV, the trigger rate is reduced by a factor of four, as shown in Fig. 6a. This comes with a loss in signal efficiency of about 20%, due to signal acceptance for the $\Delta R(\mu_1, \mu_2)$ selection, and, even more importantly, without introducing any bias or distortion in the mass distribution, as shown in Fig. 6b. Reaching a sustainable trigger rate while keeping the muon p_T threshold at the same value, 6 GeV, as in the corresponding non-topological trigger of Run 1 (2009–2013) [23] was crucial for these analyses. An increase in the p_T threshold values would have significantly cut into the signal acceptance. A similar strategy is followed for triggering $J/\psi \rightarrow ee$ events, used for example to study the performance of low- E_T electrons. Prescaled triggers requiring at least one EM TOB with $E_T > 3$ GeV and an EM TOB pair with an invariant mass between 1 and 5 GeV are used to reduce the rate and efficiently select these events [10].

A second interesting L1Topo use case from another B -physics measurement is the test of lepton-flavour universality by means of the $R_{K^{*0}}$ asymmetry analysis. The experimental signature [24] is characterised by the presence of a neutral kaon (K^{*0}) and a pair of opposite-sign collimated electrons or muons produced via radiative electroweak interactions. The main challenge in triggering on this signature at the LHC is the expected p_T of the leptons, which can be as low as a few GeV, approximately consistent with the B^0 –

K^{*0} mass difference plus the B^0 p_T . This signature is especially challenging in the electron channel, where the background rate at L1 is much higher than in the muon channel. The developed trigger strategy in the electron channel relies on the L1Topo system combining two algorithms. The first algorithm triggers on electron pairs (EM_1, EM_2) having p_T thresholds of 7 and 5 GeV respectively, and invariant mass below 9 GeV. A second algorithm targets a topology where the electrons partially or fully overlap with each other; for such cases the energy of the electrons is not fully contained in the narrow $\Delta\eta \times \Delta\phi = 0.2 \times 0.2$ geometrical L1 electron size. In order to fully measure the momenta of the electrons, thus minimising the impact of energy deposit loss, a wider jet (J) with $\Delta\eta \times \Delta\phi = 0.8 \times 0.8$ and $p_T > 15$ GeV is required to overlap, based on ΔR , with an electron (EM) with $p_T \geq 15$ GeV. These two algorithms are combined in a logical OR. As shown in Fig. 7a, the combination of the two L1Topo trigger items yields a L1 efficiency of about 40% with limited variation across the bulk of the expected signal's invariant mass distribution. The maximum L1 efficiency as a function of ΔR is about 70%, as seen in Fig. 7b; the loss of efficiency for $\Delta R > 0.4$ is driven by the L1 p_T thresholds. The combination of these two L1Topo algorithms helps to reject background events. In order to limit their rate at high luminosity, single-muon and dimuon regions-of-interest were required in the same event, with the muons expected to originate from a second b -hadron in the event.

6.2 Higgs physics

Another application of L1Topo triggers is the measurement of Higgs boson decays into two hadronically decaying τ -leptons, $H \rightarrow \tau_{\text{had}}\tau_{\text{had}}$ [25]. This analysis relies on a di- τ_{had} trigger requiring two isolated tau TOBs passing relatively low p_T thresholds of 20 GeV and 12 GeV at L1. Keeping the p_T thresholds as low as possible is very important for sensitive measurements of the Higgs boson's coupling to fermions. This can be achieved either by requiring one additional jet with $p_T > 25$ GeV in the event, which originated from vector-boson fusion produced Higgs bosons or quantum chromodynamics initial-state radiation for example, or by using a topological trigger that introduces an additional requirement on the angle between the two τ objects, $\Delta R(\tau_1, \tau_2) \leq 2.8$, to help reject a large fraction of the multi-jet background events while retaining most of the signal events. As observed in Fig. 8a, the additional jet required at L1 reduces the trigger rate by a factor of four without raising the tau TOB p_T thresholds. The reduction is similar to the rate reduction from the topological trigger requirement mentioned above. A further reduction by a factor of 1.5 is achieved when adding a second topological requirement, namely the disambiguation algorithm that requires a jet candidate with $p_T > 25$ GeV and with $\Delta R(\tau, j) > 0.1$ with respect to

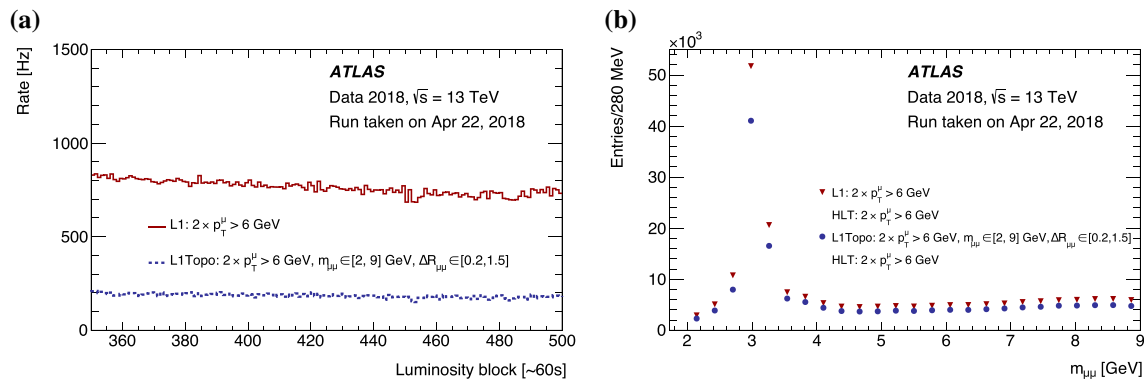


Fig. 6 Comparison of L1 dimuon triggers for muons with $p_T > 6$ GeV with and without topological requirements: **a** L1 accept rate versus luminosity block number (one luminosity block is the time interval of data recording over which the experimental conditions are assumed to be

constant, usually one minute) for an LHC pp fill with peak luminosity of $2.6 \times 10^{33} \text{ cm}^{-2}\text{s}^{-1}$; **(b)** invariant mass spectrum of the offline dimuon pair in events selected by the L1 and HLT dimuon triggers

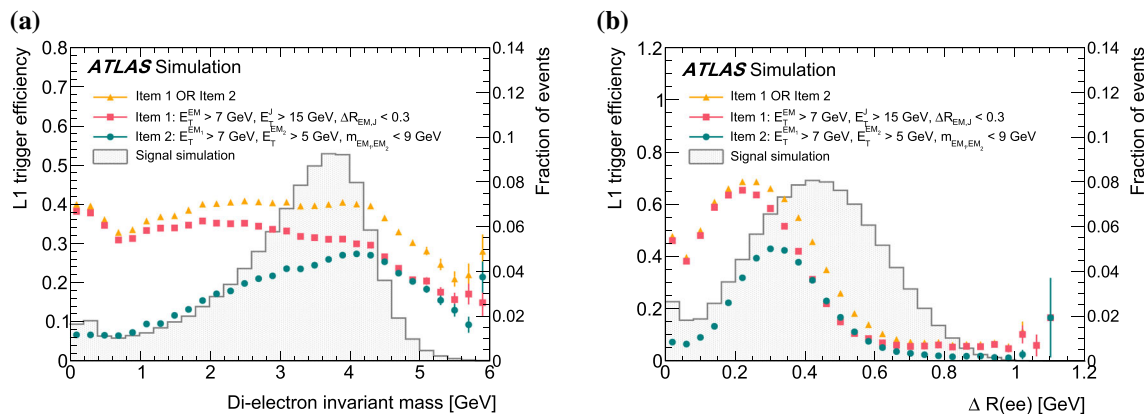


Fig. 7 Efficiency of L1Topo triggers developed for B -meson decays with di-electron final states. The efficiency is determined using non-resonant $B_d^0 \rightarrow K^{*0} e^+ e^-$ decays, and it is shown **a** as a function of the offline invariant mass of the signal electron pairs and **b** as a func-

tion of their angular separation ΔR . The L1 efficiency (coloured filled markers) is displayed separately for the two considered L1 items as well as their combination. The expected signal distribution is superimposed (filled grey histogram)

each of the τ_{had} candidates in the selected pair. Figure 8b shows the efficiency of one topological trigger relative to the non-topological di- τ_{had} trigger. Thanks to the good angular resolution of the tau TOBs, the trigger efficiency turn-on is very sharp in ΔR , making the topological trigger fully efficient for an offline selection of $\Delta R(\tau_1, \tau_2) \leq 2.6$. Typically, a requirement of $\Delta R(\tau_1, \tau_2) \leq 2.4$ is applied in the offline analysis, independently of the use of the topological trigger. Therefore, this topological algorithm does not affect the signal acceptance in the analysed phase space. These L1Topo triggers were operated without a prescale factor in the Run 2 data-taking.

Topological triggers are also useful for other Higgs analyses. For example, event hardness and invariant mass selections can be used to trigger events in which the Higgs boson is produced via vector-boson fusion. By trying to identify the two jets from the scattering process the signal acceptance of

Higgs boson decays to invisible particles can be enhanced to about 30% with respect to using the non-topological missing transverse energy requirement only. The trigger is designed to select a first jet in the central part of the detector ($|\eta| < 3.2$) and a second jet in the full detector acceptance range ($|\eta| < 4.9$) forming an invariant mass (m_{jj}) greater than 500 GeV. The pseudorapidity restriction for one of the two jets allows the rate to be reduced by a factor of five compared to using an invariant mass requirement considering all jet combinations, at the price of a 10% signal loss. Additional requirements on the pseudorapidity difference and azimuthal separation between the two jets, $\Delta\eta_{jj} > 4.0$ and $\Delta\phi_{jj} < 2.0$, are added to the HLT to further reject the multi-jet background. Figure 9a shows the trigger efficiency of the HLT trigger item seeded by the topological algorithm as a function of the maximum offline dijet mass, m_{jj}^{max} ; the HLT trigger requires $m_{jj} > 1100$ GeV, a first

jet with $p_T > 70$ GeV and $|\eta| < 3.2$, and a second jet with $p_T > 50$ GeV and $|\eta| < 4.9$. The efficiency is measured using events with at least one offline-reconstructed muon with $p_T > 27$ GeV. In addition, the events are required to have at least two anti- k_r jets [26,27] with a radius parameter $R = 0.4$, where one jet has $p_T > 90$ GeV and $|\eta| < 3.2$, while another jet has $p_T > 80$ GeV. The $\Delta\eta_{jj}$ and $\Delta\phi_{jj}$ angular requirements are also applied offline, as in the trigger requirement. The efficiency of the HLT trigger seeded by the L1Topo algorithm to select events passing the offline analysis cuts is close to 100% for events with $m_{jj}^{\max} > 1300$ GeV.

6.3 Long-lived particles

The new capabilities of the L1Topo system also allow the exploration of new ideas for unconventional signatures, such as the detection of long-lived particles (LLP). One example where L1Topo triggers are successfully used is an analysis that probes Hidden Sector models predicting decays of the Higgs boson or a new heavy neutral scalar particle Φ into neutral LLPs [28,29]. Decays of neutral LLPs in the outer layers of the electromagnetic calorimeter or in the hadronic calorimeter results in topologies characterised by displaced collimated jets with little energy deposited in the electromagnetic calorimeter and, therefore, a large hadronic to electromagnetic energy ratio, $E_{\text{HAD}}/E_{\text{EM}}$. To target these events, a L1 trigger, called high- E_T CalRatio, was designed to select narrow $\Delta\eta \times \Delta\phi = 0.2 \times 0.2$ jets with transverse energy $E_T > 60$ GeV in a combined region of the electromagnetic and hadronic calorimeters. The E_T threshold is driven by the high rates due to the pile-up conditions in Run 2; however, it strongly limits the efficiency of detecting signal events for models with m_Φ below 200 GeV. This threshold can be lowered to 30 GeV by configuring a dedicated trigger, called low- E_T CalRatio, that exploits the specific topology of these events. Considering that these jets are expected to be very collimated (with most of the energy contained in a cone of $\Delta R = 0.1$ around the jet axis), it is better to identify their calorimeter energy deposits using tau TOBs instead of jet TOBs, given their smaller area [5]. The low- E_T CalRatio trigger requires the leading- E_T tau TOB to be above 30 GeV and not to overlap with any EM TOBs with $E_T > 3$ GeV. The same requirements are also applied to the second-leading tau TOB if present. Given that the tau TOBs are reconstructed using both the electromagnetic and hadronic calorimeters while the EM TOBs are reconstructed only with the electromagnetic calorimeter, the above selection is equivalent to requiring an object with high $E_{\text{HAD}}/E_{\text{EM}}$ ratio and relies on geometrically overlapping EM and tau TOBs in the η - ϕ plane. This rejects a large fraction of the background events. Figure 9b shows the efficiency of the high- E_T and low- E_T CalRatio triggers as a function of the LLP longitudinal decay

position. The topological algorithm recovers up to about 20% of trigger efficiency for low- m_Φ hypotheses.

The capability of L1Topo to trigger on muon TOBs detected in the BC after the BC of interest is also exploited. These triggers combine the requirement of one TOB present in a given BC with the presence of a muon TOB in the following BC. They are particularly useful in searches for long-lived particles. One such example consists of requiring a jet candidate with a p_T above 50 GeV in the current BC together with a muon candidate with a p_T above 10 GeV in the following BC. The much reduced muon p_T threshold together with the also relatively low jet p_T threshold allows the efficiency to be improved by a factor of 2–3 in searches for long-lived highly ionising particles with masses above 500 GeV, with electric charge greater than one elementary charge, and with no strong interaction.

6.4 Large- R jets

Non-topological L1 jet triggers use a fixed $\Delta\eta \times \Delta\phi$ sliding-window method [5,15] with size 0.8×0.8 . These, however, fail to capture all the energy of jets with radius R larger than 0.4. The performance of this method deteriorates as the number of subjets within a jet grows, as it becomes more likely that a significant fraction of the jet energy falls outside of the selected 0.8×0.8 window. Figure 10a shows how an increase in the number of subjets reduces the trigger efficiency. The use of L1Topo provides more efficient triggering for these large- R jets. The L1Topo simple cone algorithm is designed to sum the E_T of all 0.8×0.8 jet TOBs with $E_T > 15$ GeV and a centre within a cone of $\Delta R = 1$. The obtained E_T sum, representing the energy of the large- R jet, is required to be larger than 111 GeV; this value is chosen to result in a trigger rate equals to that of the non-topological 100 GeV jet trigger. Figure 10b shows the L1Topo simple cone algorithm trigger efficiency for events with jets of various numbers of subjets. The comparison of Fig. 10a, b shows that the L1Topo simple cone is able to reduce by up to 30 GeV the p_T value at which the trigger becomes fully efficient for events with jets of multiple subjets. It can also be observed that the L1Topo trigger efficiency for events with jets of one single subjet is worse than that corresponding to the single jet trigger. This is due to the increase in the jet E_T requirement from 100 GeV to 111 GeV. However, this small increase in threshold does not affect the offline selection efficiency, as the HLT triggers of single jets require a much higher E_T , above 400 GeV, thus removing the events under the L1Topo trigger efficiency turn-on. In contrast, the HLT triggers aiming at final states involving the production of multiple hadronically decaying massive particles (dibosons, $t\bar{t}$, etc.) can use mass cuts to strongly suppress multi-jet events, the dominant source of a high trigger rate, and the minimum jet E_T requirement can thus be relaxed to 330 GeV. This threshold is well above the

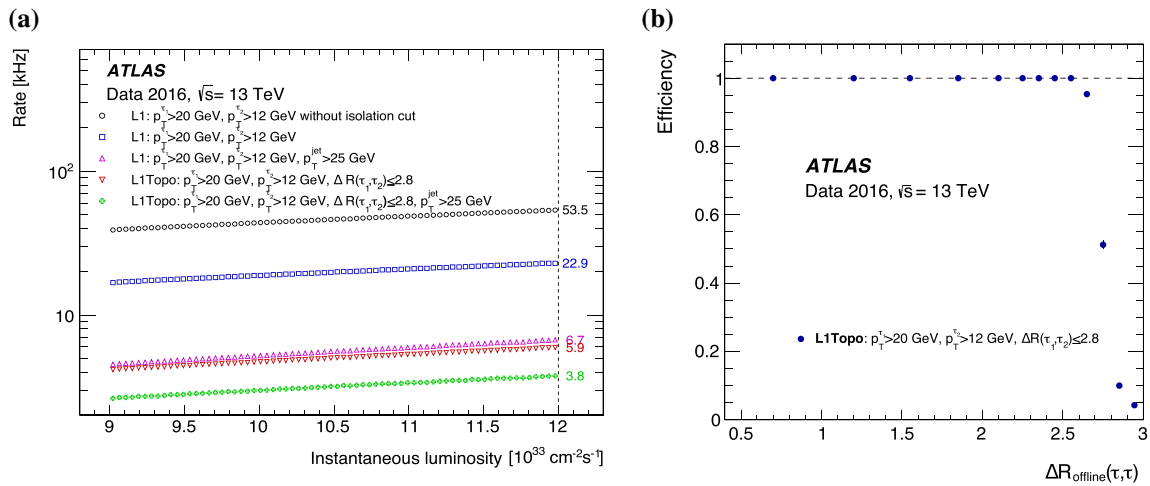


Fig. 8 **a** Comparison of the L1 rate as a function of the instantaneous luminosity for di- τ_{had} triggers with (open red triangles) and without (open blue boxes) topological requirements; the same figure also shows the L1 rate as a function of the instantaneous luminosity for di- τ_{had} triggers with (open green crosses) or without (open pink triangles) the requirement of an additional jet; the L1 rates corresponding to an

instantaneous luminosity of $12 \times 10^{33} \text{ cm}^{-2} \text{ s}^{-1}$ are also displayed. **b** Efficiency of the topological di- τ_{had} trigger for events passing the non-topological trigger as a function of the $\Delta R(\tau_1, \tau_2)$ between the two τ -leptons. Algorithms requiring an additional jet also apply the selection $\Delta R(\tau, j) > 0.1$ in order to prevent double counting of tau and jet TOBs

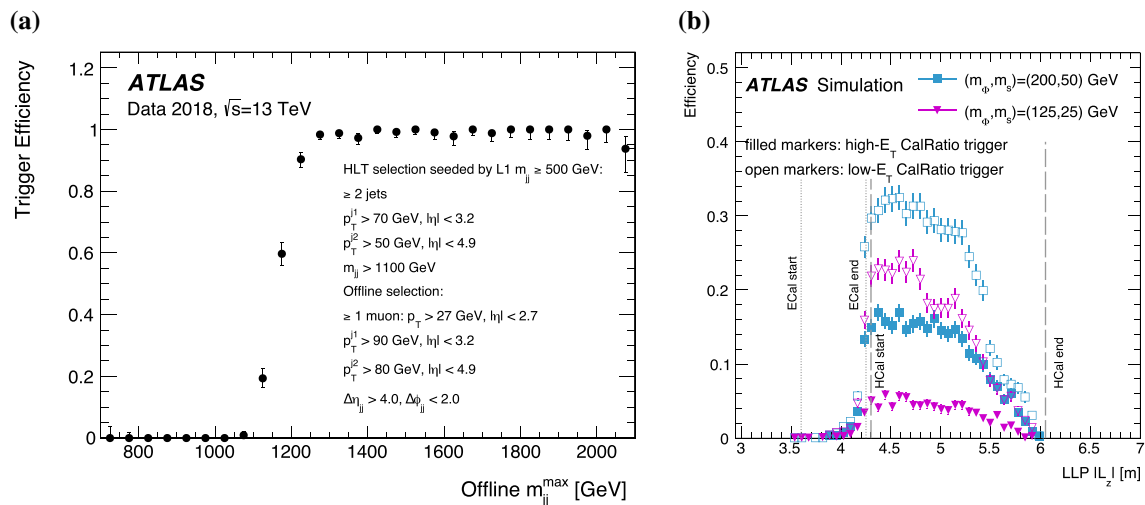


Fig. 9 **a** Efficiency of the HLT dijet trigger as a function of the maximum offline dijet mass. The L1 topological algorithm used in this trigger requires the dijet invariant mass to be above 500 GeV and at least one of the two jets to be in the central part of the detector ($|\eta| < 3.2$). The efficiency is measured using events that are selected using a single muon trigger with $p_T > 27$ GeV. In addition, events are required to have at least two jets with $E_T > 80$ and 90 GeV, respectively. Angu-

lar requirements between the jets are also applied offline. **b** Efficiency of the high- E_T non-topological CalRatio trigger (filled markers) and of the low- E_T topological CalRatio trigger (open markers) as a function of the absolute value of the LLP longitudinal decay position, L_z . Different mass hypotheses for the signal models are represented in different colours. The grey dotted (dashed) lines show the start and end z -positions of the electromagnetic (hadronic) calorimeter

point at which the L1Topo cone algorithm is fully efficient for jets with subjet multiplicities of three or more, while being at the edge of the efficiency plateau for the traditional 0.8×0.8 L1 jet algorithm. In 2018, the L1Topo simple cone algorithm became the default L1 large- R jet algorithm used to seed all HLT triggers targeting boosted hadronically decaying massive particles.

7 Conclusions

The L1 topological processor provides the ATLAS L1 trigger system with the capability of applying kinematic selections among muon and calorimeter-based trigger objects to substantially reduce the L1-accept trigger rate, while maintaining high signal acceptance, at instantaneous luminosi-

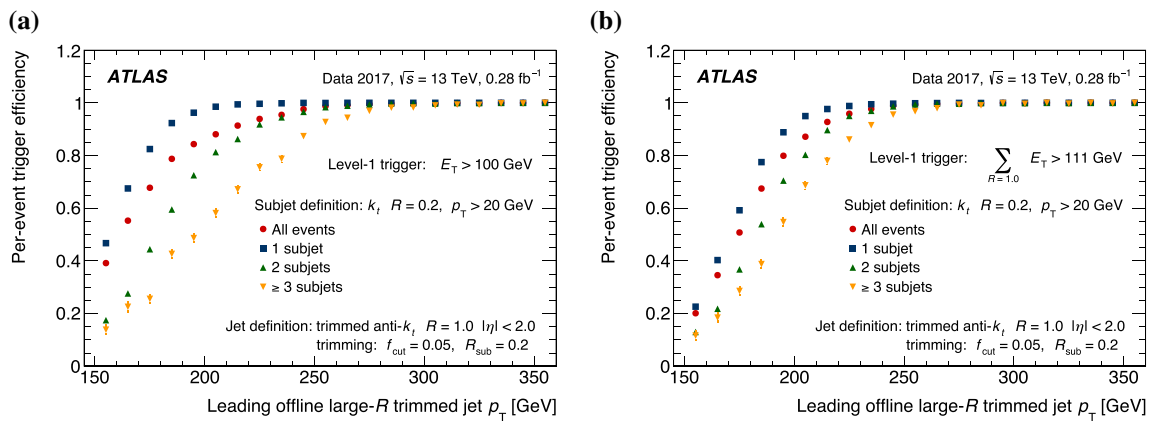


Fig. 10 Trigger efficiency curves as a function of the leading offline trimmed jet p_T [30] for events with jets of one, two or more than two subjects selected using **a** the standard jet sliding-window algorithm and **b** the L1Topo simple cone algorithm

ties up to $2.1 \times 10^{34} \text{ cm}^{-2} \text{ s}^{-1}$. This new capability became available for the ATLAS physics programme during LHC Run 2. The topological triggers are particularly important for physics analyses making use of low- p_T objects, such as in Higgs boson and B -physics measurements. The L1Topo system also makes it possible to trigger on objects from consecutive BCs. The system was successfully installed and commissioned in 2016 and operated during pp physics data-taking in 2017 and 2018. Simulation, validation and monitoring tools have been crucial for the commissioning and monitoring of the system.

Acknowledgements We thank CERN for the very successful operation of the LHC, as well as the support staff from our institutions without whom ATLAS could not be operated efficiently. We acknowledge the support of ANPCyT, Argentina; YerPhI, Armenia; ARC, Australia; BMWFW and FWF, Austria; ANAS, Azerbaijan; SSTC, Belarus; CNPq and FAPESP, Brazil; NSERC, NRC and CFI, Canada; CERN; ANID, Chile; CAS, MOST and NSFC, China; COLCIENCIAS, Colombia; MSMT CR, MPO CR and VSC CR, Czech Republic; DNRF and DNSRC, Denmark; IN2P3-CNRS and CEA-DRF/IRFU, France; SRNSFG, Georgia; BMBF, HGF and MPG, Germany; GSRT, Greece; RGC and Hong Kong SAR, China; ISF and Benozio Center, Israel; INFN, Italy; MEXT and JSPS, Japan; CNRST, Morocco; NWO, Netherlands; RCN, Norway; MNiSW and NCN, Poland; FCT, Portugal; MNE/IFA, Romania; JINR; MES of Russia and NRC KI, Russian Federation; MESTD, Serbia; MSSR, Slovakia; ARRS and MIZŠ, Slovenia; DST/NRF, South Africa; MICINN, Spain; SRC and Wallenberg Foundation, Sweden; SERI, SNSF and Cantons of Bern and Geneva, Switzerland; MOST, Taiwan; TAEK, Turkey; STFC, United Kingdom; DOE and NSF, United States of America. In addition, individual groups and members have received support from BCKDF, CANARIE, Compute Canada, CRC and IVADO, Canada; Beijing Municipal Science & Technology Commission, China; COST, ERC, ERDF, Horizon 2020 and Marie Skłodowska-Curie Actions, European Union; Investissements d’Avenir Labex, Investissements d’Avenir Idex and ANR, France; DFG and AvH Foundation, Germany; Herakleitos, Thales and Aristeia programmes co-financed by EU-ESF and the Greek NSRF, Greece; BSF-NSF and GIF, Israel; La Caixa Banking Foundation, CERCA Programme Generalitat de Catalunya and PROMETEO and GenT Programmes Generalitat Valenciana, Spain; Göran Gustafssons Stiftelse,

Sweden; The Royal Society and Leverhulme Trust, United Kingdom. The crucial computing support from all WLCG partners is acknowledged gratefully, in particular from CERN, the ATLAS Tier-1 facilities at TRIUMF (Canada), NDGF (Denmark, Norway, Sweden), CC-IN2P3 (France), KIT/GridKA (Germany), INFN-CNAF (Italy), NL-T1 (Netherlands), PIC (Spain), ASGC (Taiwan), RAL (UK) and BNL (USA), the Tier-2 facilities worldwide and large non-WLCG resource providers. Major contributors of computing resources are listed in Ref. [31].

Data Availability Statement This manuscript has no associated data in a data repository. [Authors’ comment: All ATLAS scientific output is published in journals, and preliminary results are made available in Conference Notes. All are openly available, without restriction on use by external parties beyond copyright law and the standard conditions agreed by CERN. Data associated with journal publications are also made available: tables and data from plots (e.g. cross section values, likelihood profiles, selection efficiencies, cross section limits, ...) are stored in appropriate repositories such as HEPDATA (<http://hepdata.cedar.ac.uk/>). ATLAS also strives to make additional material related to the paper available that allows a reinterpretation of the data in the context of new theoretical models. For example, an extended encapsulation of the analysis is often provided for measurements in the framework of RIVET (<http://rivet.hepforge.org/>). The above sentence is taken from the ATLAS Data Access Policy. Please make reference to it saying that it is a public document that can be downloaded from here: <http://opendata.cern.ch/record/413> [opendata.cern.ch].]

Open Access This article is licensed under a Creative Commons Attribution 4.0 International License, which permits use, sharing, adaptation, distribution and reproduction in any medium or format, as long as you give appropriate credit to the original author(s) and the source, provide a link to the Creative Commons licence, and indicate if changes were made. The images or other third party material in this article are included in the article’s Creative Commons licence, unless indicated otherwise in a credit line to the material. If material is not included in the article’s Creative Commons licence and your intended use is not permitted by statutory regulation or exceeds the permitted use, you will need to obtain permission directly from the copyright holder. To view a copy of this licence, visit <http://creativecommons.org/licenses/by/4.0/>.
Funded by SCOAP³.

References

1. ATLAS Collaboration, The ATLAS Experiment at the CERN Large Hadron Collider. JINST **3**, S08003 (2008)
2. ATLAS Collaboration, Operation of the ATLAS trigger system in Run 2. JINST **15**, P10004 (2020). [arXiv:2007.12539](https://arxiv.org/abs/2007.12539) [physics.ins-det]
3. ATLAS Collaboration, Performance of the ATLAS trigger system in 2015. Eur. Phys. J. C **77**, 317 (2017). [arXiv:1611.09661](https://arxiv.org/abs/1611.09661) [hep-ex]
4. ATLAS TDAQ Collaboration, The ATLAS Data Acquisition and High Level Trigger system. JINST **11**, P06008 (2016)
5. R. Achenbach et al., The ATLAS Level-1 Calorimeter Trigger. JINST **3**, P03001 (2008)
6. ATLAS Collaboration, Performance of the ATLAS muon triggers in Run 2. JINST **15**, P09015 (2020). [arXiv:2004.13447](https://arxiv.org/abs/2004.13447) [hep-ex]
7. ATCA specifications, (2021). <https://www.picmg.org/openstandards/advancedtca/>
8. Xilinx Virtex-7 FPGA, (2021). <https://www.xilinx.com/products/silicon-devices/fpga/virtex-7.html>
9. Xilinx Kintex-7 FPGA, (2021). <https://www.xilinx.com/products/silicon-devices/fpga/kintex-7.html>
10. ATLAS Collaboration, Performance of electron and photon triggers in ATLAS during LHC Run 2. Eur. Phys. J. C **80**, 47 (2020). [arXiv:1909.00761](https://arxiv.org/abs/1909.00761) [hep-ex]
11. ATLAS Collaboration, Performance of the missing transverse momentum triggers for the ATLAS detector during Run-2 data taking. JHEP **08**, 080 (2020). [arXiv:2005.09554](https://arxiv.org/abs/2005.09554) [hep-ex]
12. Avago miniPODs specifications, (2021). <https://www.broadcom.com/products/fiber-optic-modules/components/networking/embedded-optical-modules/minipod/afbr-814vxyz>, <https://www.broadcom.com/products/fiber-optic-modules/components/networking/embeddedoptical-modules/minipod/afbr-824vxyz>
13. ATLAS Collaboration, ATLAS level-1 trigger: Technical Design Report, Technical design report (ATLAS, CERN, Geneva, 1998). <https://cds.cern.ch/record/381429>
14. IEEE Standard for VHDL Language Reference Manual, IEEE Std 1076-2019 (2019). <https://standards.ieee.org/standard/1076-2019.html>
15. W. Lampl et al., Calorimeter Clustering Algorithms: Description and Performance, ATL-LARGPUB-2008-002 (2008). <https://cds.cern.ch/record/1099735>
16. ATLAS Collaboration, Trigger Menu in 2016, ATL-DAQ-PUB-2017-001 (2017). <https://cds.cern.ch/record/2242069>
17. ATLAS Collaboration, Trigger Menu in 2017, ATL-DAQ-PUB-2018-002 (2018). <https://cds.cern.ch/record/2625986>
18. ATLAS Collaboration, Trigger Menu in 2018, ATL-DAQ-PUB-2019-001 (2019). <https://cds.cern.ch/record/2693402>
19. D. Guadagnoli, Flavor anomalies on the eve of the Run-2 verdict. Mod. Phys. Lett. A **32**, 1730006 (2017). [arXiv:1703.02804](https://arxiv.org/abs/1703.02804) [hep-ph]
20. ATLAS Collaboration, Fast TracKer (FTK) Technical Design Report, tech. rep. CERN-LHCC-2013-007. ATLAS-TDR-021, ATLAS Fast Tracker Technical Design Report (2013). <https://cds.cern.ch/record/1552953>
21. ATLAS Collaboration, Letter of Intent for the Phase-I Upgrade of the ATLAS Experiment, tech. rep. CERN-LHCC-2011-012. LHCC-I-020, CERN (2011). <http://cds.cern.ch/record/1402470>
22. ATLAS Collaboration, Measurement of the CP-violating phase ϕ_s in $B_s^0 \rightarrow J/\psi\phi$ decays in ATLAS at 13 TeV (2020). [arXiv:2001.07115](https://arxiv.org/abs/2001.07115) [hep-ex]
23. ATLAS Collaboration, Performance of the ATLAS muon trigger in pp collisions at $\sqrt{s} = 8 TeV$. Eur. Phys. J. C **75**, 120 (2015). [arXiv:1408.3179](https://arxiv.org/abs/1408.3179) [hep-ex]
24. LHCb Collaboration, Test of lepton universality with $B^0 \rightarrow K^{*0}l^+l^-$ decays. JHEP **08**, 055 (2017). [arXiv:1705.05802](https://arxiv.org/abs/1705.05802) [hep-ex]
25. ATLAS Collaboration, The ATLAS Tau Trigger in Run 2, ATLAS-CONF-2017-061 (2017). <https://cds.cern.ch/record/2274201>
26. M. Cacciari, G.P. Salam, G. Soyez, FastJet user manual. Eur. Phys. J. C **72**, 1896 (2012). [arXiv:1111.6097](https://arxiv.org/abs/1111.6097) [hep-ph]
27. M. Cacciari, G.P. Salam, G. Soyez, The anti- k_r jet clustering algorithm. JHEP **04**, 063 (2008). [arXiv:0802.1189](https://arxiv.org/abs/0802.1189) [hep-ph]
28. ATLAS Collaboration, Search for long-lived neutral particles in pp collisions at $\sqrt{s} = 13 TeV$ that decay into displaced hadronic jets in the ATLAS calorimeter. Eur. Phys. J. C **79**, 481 (2019). [arXiv:1902.03094](https://arxiv.org/abs/1902.03094) [hep-ex]
29. ATLAS Collaboration, Triggers for displaced decays of long-lived neutral particles in the ATLAS detector. JINST **8**, P07015 (2013). [arXiv:1305.2284](https://arxiv.org/abs/1305.2284) [hep-ex]
30. D. Krohn, J. Thaler, L.-T. Wang, Jet trimming. JHEP **02**, 084 (2010). [arXiv:0912.1342](https://arxiv.org/abs/0912.1342) [hep-ph]
31. ATLAS Collaboration, ATLAS Computing Acknowledgements, ATL-SOFT-PUB-2020-001 (2020). <https://cds.cern.ch/record/2717821>

ATLAS Collaboration

G. Aad¹⁰¹, B. Abbott¹²⁷, D. C. Abbott¹⁰², A. Abed Abud³⁶, K. Abeling⁵³, D. K. Abhayasinghe⁹³, S. H. Abidi²⁹, O. S. AbouZeid⁴⁰, N. L. Abraham¹⁵⁵, H. Abramowicz¹⁶⁰, H. Abreu¹⁵⁹, Y. Abulaiti⁶, A. C. Abusleme Hoffman^{145a}, B. S. Acharya^{66a,66b,p}, B. Achkar⁵³, L. Adam⁹⁹, C. Adam Bourdarios⁵, L. Adamczyk^{83a}, L. Adamek¹⁶⁵, J. Adelman¹²⁰, A. Adiguzel^{12c,ae}, S. Adorni⁵⁴, T. Adye¹⁴², A. A. Affolder¹⁴⁴, Y. Afik¹⁵⁹, C. Agapopoulou⁶⁴, M. N. Agaras³⁸, A. Aggarwal¹¹⁸, C. Agheorghiesei^{27c}, J. A. Aguilar-Saavedra^{138f,138a,ad}, A. Ahmad³⁶, F. Ahmadov⁷⁹, W. S. Ahmed¹⁰³, X. Ai⁴⁶, G. Aielli^{73a,73b}, S. Akatsuka⁸⁵, M. Akbiyik⁹⁹, T. P. A. Åkesson⁹⁶, E. Akilli⁵⁴, A. V. Akimov¹¹⁰, K. Al Khoury³⁹, G. L. Alberghi^{23a,23b}, J. Albert¹⁷⁴, M. J. Alconada Verzini¹⁶⁰, S. Alderweireldt³⁶, M. Aleksa³⁶, I. N. Aleksandrov⁷⁹, C. Alexa^{27b}, T. Alexopoulos¹⁰, A. Alfonsi¹¹⁹, F. Alfonsi^{23a,23b}, M. Alhroob¹²⁷, B. Ali¹⁴⁰, S. Ali¹⁵⁷, M. Aliev¹⁶⁴, G. Alimonti^{68a}, C. Allaire³⁶, B. M. M. Allbrooke¹⁵⁵, P. P. Allport²¹, A. Aloisio^{69a,69b}, F. Alonso⁸⁸, C. Alpigiani¹⁴⁷, E. Alunno Camelia^{73a,73b}, M. Alvarez Estevez⁹⁸, M. G. Alvigi^{69a,69b}, Y. Amaral Coutinho^{80b}, A. Ambler¹⁰³, L. Ambroz¹³³, C. Amelung³⁶, D. Amidei¹⁰⁵, S. P. Amor Dos Santos^{138a}, S. Amoroso⁴⁶, C. S. Amrouche⁵⁴, C. Anastopoulos¹⁴⁸, N. Andari¹⁴³, T. Andeen¹¹, J. K. Anders²⁰, S. Y. Andreato^{45a,45b}, A. Andreazza^{68a,68b}, V. Andrei^{61a}, S. Angelidakis⁹, A. Angerami³⁹, A. V. Anisenkov^{121a,121b}, A. Annovi^{71a}, C. Antel⁵⁴, M. T. Anthony¹⁴⁸, E. Antipov¹²⁸, M. Antonelli⁵¹, D. J. A. Antrim¹⁸, F. Anulli^{72a}, M. Aoki⁸¹, J. A. Aparisi Pozo¹⁷², M. A. Aparo¹⁵⁵, L. Aperio Bella⁴⁶, N. Aranzabal³⁶, V. Araujo Ferraz^{80a}, C. Arcangeletti⁵¹, A. T. H. Arce⁴⁹, J.-F. Arguin¹⁰⁹, S. Argyropoulos⁵², J.-H. Arling⁴⁶, A. J. Armbruster³⁶, A. Armstrong¹⁶⁹, O. Arnaez¹⁶⁵, H. Arnold³⁶, Z. P. Arrubarrena Tame¹¹³, G. Artoni¹³³, S. Artz⁹⁹, H. Asada¹¹⁶, K. Asai¹²⁵, S. Asai¹⁶², N. Asbah⁵⁹, E. M. Asimakopoulou¹⁷⁰, L. Asquith¹⁵⁵, J. Assahsah^{35e}, K. Assamagan²⁹, R. Astalos^{28a}, R. J. Atkin^{33a}, M. Atkinson¹⁷¹, N. B. Atlay¹⁹, H. Atmani⁶⁴, P. A. Atmasiddha¹⁰⁵, K. Augsten¹⁴⁰, V. A. Austrup¹⁸⁰, G. Avolio³⁶, M. K. Ayoub^{15c}, G. Azuelos^{109,al}, D. Babal^{28a}, H. Bachacou¹⁴³, K. Bachas¹⁶¹, F. Backman^{45a,45b}, P. Bagnaia^{72a,72b}, M. Bahmani⁸⁴, H. Bahrasemani¹⁵¹, A. J. Bailey¹⁷², V. R. Bailey¹⁷¹, J. T. Baines¹⁴², C. Bakalis¹⁰, O. K. Baker¹⁸¹, P. J. Bakker¹¹⁹, E. Bakos¹⁶, D. Bakshi Gupta⁸, S. Balaji¹⁵⁶, R. Balasubramanian¹¹⁹, E. M. Baldin^{121a,121b}, P. Balek¹⁷⁸, F. Balli¹⁴³, W. K. Balunas¹³³, J. Balz⁹⁹, E. Banas⁸⁴, M. Bandieramonte¹³⁷, A. Bandyopadhyay¹⁹, L. Barak¹⁶⁰, W. M. Barbe³⁸, E. L. Barberio¹⁰⁴, D. Barberis^{55a,55b}, M. Barbero¹⁰¹, G. Barbour⁹⁴, K. N. Barends^{33a}, T. Barillari¹¹⁴, M.-S. Barisits³⁶, J. Barkeloo¹³⁰, T. Barklow¹⁵², B. M. Barnett¹⁴², R. M. Barnett¹⁸, Z. Barnovska-Blenessy^{60a}, A. Baroncelli^{60a}, G. Barone²⁹, A. J. Barr¹³³, L. Barranco Navarro^{45a,45b}, F. Barreiro⁹⁸, J. Barreiro Guimarães da Costa^{15a}, U. Barron¹⁶⁰, S. Barsov¹³⁶, F. Bartels^{61a}, R. Bartoldus¹⁵², G. Bartolini¹⁰¹, A. E. Barton⁸⁹, P. Bartos^{28a}, A. Basalae⁴⁶, A. Basan⁹⁹, I. Bashta^{74a,74b}, A. Bassalat^{64,ai}, M. J. Basso¹⁶⁵, C. R. Basson¹⁰⁰, R. L. Bates⁵⁷, S. Batlamous^{35f}, J. R. Batley³², B. Batool¹⁵⁰, M. Battaglia¹⁴⁴, M. Bauce^{72a,72b}, F. Bauer^{143,*}, P. Bauer²⁴, B. Bauss⁹⁹, H. S. Bawa³¹, A. Bayirli^{12c}, J. B. Beacham⁴⁹, T. Beau¹³⁴, P. H. Beauchemin¹⁶⁸, F. Becherer⁵², P. Bechtle²⁴, H. P. Beck^{20,r}, K. Becker¹⁷⁶, C. Becot⁴⁶, A. J. Beddall^{12a}, V. A. Bednyakov⁷⁹, C. P. Bee¹⁵⁴, T. A. Beermann¹⁸⁰, M. Begalli^{80b}, M. Begel²⁹, A. Behera¹⁵⁴, J. K. Behr⁴⁶, J. F. Beirer^{36,53}, F. Beisiegel²⁴, M. Belfkir⁵, G. Bella¹⁶⁰, L. Bellagamba^{23b}, A. Bellerive³⁴, P. Bellos²¹, K. Beloborodov^{121a,121b}, K. Belotskiy¹¹¹, N. L. Belyaev¹¹¹, D. Benchekroun^{35a}, N. Benekos¹⁰, Y. Benhammou¹⁶⁰, D. P. Benjamin⁶, M. Benoit²⁹, J. R. Bensinger²⁶, S. Bentvelsen¹¹⁹, L. Beresford¹³³, M. Beretta⁵¹, D. Berge¹⁹, E. Bergeaas Kuutmann¹⁷⁰, N. Berger⁵, B. Bergmann¹⁴⁰, L. J. Bergsten²⁶, J. Beringer¹⁸, S. Berlendis⁷, G. Bernardi¹³⁴, C. Bernius¹⁵², F. U. Bernlochner²⁴, T. Berry⁹³, P. Berta⁴⁶, A. Berthold⁴⁸, I. A. Bertram⁸⁹, O. Bessidskaia Bylund¹⁸⁰, S. Bethke¹¹⁴, A. Betti⁴², A. J. Bevan⁹², S. Bhatta¹⁵⁴, D. S. Bhattacharya¹⁷⁵, P. Bhattarai²⁶, V. S. Bhopatkar⁶, R. Bi¹³⁷, R. M. Bianchi¹³⁷, O. Biebel¹¹³, R. Bielski³⁶, K. Bierwagen⁹⁹, N. V. Biesuz^{71a,71b}, M. Biglietti^{74a}, T. R. V. Billoud¹⁴⁰, M. Bindi⁵³, A. Bingul^{12d}, C. Bini^{72a,72b}, S. Biondi^{23a,23b}, C. J. Birch-sykes¹⁰⁰, G. A. Bird^{21,142}, M. Birman¹⁷⁸, T. Bisanz³⁶, J. P. Biswal³, D. Biswas^{179,k}, A. Bitadze¹⁰⁰, C. Bittrich⁴⁸, K. Björke¹³², T. Blazek^{28a}, I. Bloch⁴⁶, C. Blocker²⁶, A. Blue⁵⁷, U. Blumenschein⁹², G. J. Bobbink¹¹⁹, V. S. Bobrovnikov^{121a,121b}, D. Bogavac¹⁴, A. G. Bogdanchikov^{121a,121b}, C. Bohm^{45a}, V. Boisvert⁹³, P. Bokan⁴⁶, T. Bold^{83a}, M. Bomben¹³⁴, M. Bona⁹², J. S. Bonilla¹³⁰, M. Boonekamp¹⁴³, C. D. Booth⁹³, A. G. Borbély⁵⁷, H. M. Borecka-Bielska¹⁰⁹, L. S. Borgna⁹⁴, G. Borissov⁸⁹, D. Bortoletto¹³³, D. Boscherini^{23b}, M. Bosman¹⁴, J. D. Bossio Sola¹⁰³, K. Bouaouda^{35a}, J. Boudreau¹³⁷, E. V. Bouhova-Thacker⁸⁹, D. Boumediene³⁸, R. Bouquet¹³⁴, A. Boveia¹²⁶, J. Boyd³⁶, D. Boye²⁹, I. R. Boyko⁷⁹, A. J. Bozson⁹³, J. Bracinik²¹,

J. I. Djuvsland¹⁷, M. A. B. Do Vale¹⁴⁶, M. Dobre^{27b}, D. Dodsworth²⁶, C. Doglioni⁹⁶, J. Dolejsi¹⁴¹, Z. Dolezal¹⁴¹, M. Donadelli^{80c}, B. Dong^{60c}, J. Donini³⁸, A. D'onofrio^{15c}, M. D'Onofrio⁹⁰, J. Dopke¹⁴², A. Doria^{69a}, M. T. Dova⁸⁸, A. T. Doyle⁵⁷, E. Drechsler¹⁵¹, E. Dreyer¹⁵¹, T. Dreyer⁵³, A. S. Drobac¹⁶⁸, D. Du^{60b}, T. A. du Pree¹¹⁹, Y. Duan^{60d}, F. Dubinin¹¹⁰, M. Dubovsky^{28a}, A. Dubreuil⁵⁴, E. Duchovni¹⁷⁸, G. Duckeck¹¹³, O. A. Ducu^{36,27b}, D. Duda¹¹⁴, A. Dudarev³⁶, A. C. Dudder⁹⁹, M. D'uffizi¹⁰⁰, L. Duflot⁶⁴, M. Dührssen³⁶, C. Dülsen¹⁸⁰, M. Dumancic¹⁷⁸, A. E. Dumitriu^{27b}, M. Dunford^{61a}, S. Dungs⁴⁷, A. Duperrin¹⁰¹, H. Duran Yildiz^{4a}, M. Düren⁵⁶, A. Durglishvili^{158b}, B. Dutta⁴⁶, D. Duvnjak¹, G. I. Dyckes¹³⁵, M. Dyndal^{83a}, S. Dysch¹⁰⁰, B. S. Dziedzic⁸⁴, B. Eckerova^{28a}, M. G. Eggleston⁴⁹, E. Egidio Purcino De Souza^{80b}, L. F. Ehrke⁵⁴, T. Eifert⁸, G. Eigen¹⁷, K. Einsweiler¹⁸, T. Ekelof¹⁷⁰, H. El Jarrari^{35f}, A. El Moussaouy^{35a}, V. Ellajosyula¹⁷⁰, M. Ellert¹⁷⁰, F. Ellinghaus¹⁸⁰, A. A. Elliot⁹², N. Ellis³⁶, J. Elmsheuser²⁹, M. Elsing³⁶, D. Emeliyanov¹⁴², A. Emerman³⁹, Y. Enari¹⁶², J. Erdmann⁴⁷, A. Ereditato²⁰, P. A. Erland⁸⁴, M. Errenst¹⁸⁰, M. Escalier⁶⁴, C. Escobar¹⁷², O. Estrada Pastor¹⁷², E. Etzion¹⁶⁰, G. Evans^{138a}, H. Evans⁶⁵, M. O. Evans¹⁵⁵, A. Ezhilov¹³⁶, F. Fabbri⁵⁷, L. Fabbri^{23a,23b}, V. Fabiani¹¹⁸, G. Facini¹⁷⁶, R. M. Fakhrutdinov¹²², S. Falciano^{72a}, P. J. Falke²⁴, S. Falke³⁶, J. Faltova¹⁴¹, Y. Fan^{15a}, Y. Fang^{15a}, Y. Fang^{15a}, G. Fanourakis⁴⁴, M. Fanti^{68a,68b}, M. Faraj^{60c}, A. Farbin⁸, A. Farilla^{74a}, E. M. Farina^{70a,70b}, T. Farooque¹⁰⁶, S. M. Farrington⁵⁰, P. Farthouat³⁶, F. Fassi^{35f}, D. Fassouliotis⁹, M. Fauci Giannelli^{73a,73b}, W. J. Fawcett³², L. Fayard⁶⁴, O. L. Fedin^{136,q}, A. Fehr²⁰, M. Feickert¹⁷¹, L. Felgioni¹⁰¹, A. Fell¹⁴⁸, C. Feng^{60b}, M. Feng⁴⁹, M. J. Fenton¹⁶⁹, A. B. Fenyuk¹²², S. W. Ferguson⁴³, J. Ferrando⁴⁶, A. Ferrari¹⁷⁰, P. Ferrari¹¹⁹, R. Ferrari^{70a}, D. Ferrere⁵⁴, C. Ferretti¹⁰⁵, F. Fiedler⁹⁹, A. Filipčić⁹¹, F. Filthaut¹¹⁸, K. D. Finelli²⁵, M. C. N. Fiolhais^{138a,138c,a}, L. Fiorini¹⁷², F. Fischer¹¹³, J. Fischer⁹⁹, W. C. Fisher¹⁰⁶, T. Fitschen²¹, I. Fleck¹⁵⁰, P. Fleischmann¹⁰⁵, T. Flick¹⁸⁰, B. M. Flierl¹¹³, L. Flores¹³⁵, L. R. Flores Castillo^{62a}, F. M. Follega^{75a,75b}, N. Fomin¹⁷, J. H. Foo¹⁶⁵, G. T. Forcolin^{75a,75b}, B. C. Forland⁶⁵, A. Formica¹⁴³, F. A. Förster¹⁴, A. C. Forti¹⁰⁰, E. Fortin¹⁰¹, M. G. Foti¹³³, D. Fournier⁶⁴, H. Fox⁸⁹, P. Francavilla^{71a,71b}, S. Francescato^{72a,72b}, M. Franchini^{23a,23b}, S. Franchino^{61a}, D. Francis³⁶, L. Franco⁵, L. Franconi²⁰, M. Franklin⁵⁹, G. Frattari^{72a,72b}, P. M. Freeman²¹, B. Freund¹⁰⁹, W. S. Freund^{80b}, E. M. Freundlich⁴⁷, D. C. Frizzell¹²⁷, D. Froidevaux³⁶, J. A. Frost¹³³, Y. Fu^{60a}, M. Fujimoto¹²⁵, E. Fullana Torregrosa¹⁷², T. Fusayasu¹¹⁵, J. Fuster¹⁷², A. Gabrielli^{23a,23b}, A. Gabrielli³⁶, P. Gadov⁴⁶, G. Gagliardi^{55b,55a}, L. G. Gagnon¹⁸, G. E. Gallardo¹³³, E. J. Gallas¹³³, B. J. Gallop¹⁴², R. Gamboa Goni⁹², K. K. Gan¹²⁶, S. Ganguly¹⁷⁸, J. Gao^{60a}, Y. Gao⁵⁰, Y. S. Gao^{31,n}, F. M. Garay Walls^{145a}, C. García¹⁷², J. E. García Navarro¹⁷², J. A. García Pascual^{15a}, M. Garcia-Sciveres¹⁸, R. W. Gardner³⁷, D. Garg⁷⁷, S. Gargiulo⁵², C. A. Garner¹⁶⁵, V. Garonne¹³², S. J. Gasiorowski¹⁴⁷, P. Gaspar^{80b}, G. Gaudio^{70a}, P. Gauzzi^{72a,72b}, I. L. Gavrilenko¹¹⁰, A. Gavriilyuk¹²³, C. Gay¹⁷³, G. Gaycken⁴⁶, E. N. Gazis¹⁰, A. A. Geanta^{27b}, C. M. Gee¹⁴⁴, C. N. P. Gee¹⁴², J. Geisen⁹⁶, M. Geisen⁹⁹, C. Gemme^{55b}, M. H. Genest⁵⁸, C. Geng¹⁰⁵, S. Gentile^{72a,72b}, S. George⁹³, T. Gerasis⁴⁴, D. Gerbaudo¹⁴, L. O. Gerlach⁵³, P. Gessinger-Befurt⁹⁹, G. Gessner⁴⁷, M. Ghasemi Bostanabad¹⁷⁴, M. Ghneimat¹⁵⁰, A. Ghosh¹⁶⁹, A. Ghosh⁷⁷, B. Giacobbe^{23b}, S. Giagu^{72a,72b}, N. Giangiacomi¹⁶⁵, P. Giannetti^{71a}, A. Giannini^{69a,69b}, S. M. Gibson⁹³, M. Gignac¹⁴⁴, D. T. Gil^{83b}, B. J. Gilbert³⁹, D. Gillberg³⁴, G. Gilles¹⁸⁰, N. E. K. Gillwald⁴⁶, D. M. Gingrich^{3,al}, M. P. Giordani^{66a,66c}, P. F. Giraud¹⁴³, G. Giugliarelli^{66a,66c}, D. Giugni^{68a}, F. Giuli^{73a,73b}, S. Gkaitatzis¹⁶¹, I. Gkialas^{9,i}, E. L. Gkoukousis¹⁴, P. Gkoutoumis¹⁰, L. K. Gladilin¹¹², C. Glasman⁹⁸, G. R. Gledhill¹³⁰, M. Glisic¹³⁰, I. Gnesi^{41b,d}, M. Goblirsch-Kolb²⁶, D. Godin¹⁰⁹, S. Goldfarb¹⁰⁴, T. Golling⁵⁴, D. Golubkov¹²², A. Gomes^{138a,138b}, R. Goncalves Gama⁵³, R. Gonçalves^{138a,138c}, G. Gonella¹³⁰, L. Gonella²¹, A. Gongadze⁷⁹, F. Gonnella²¹, J. L. Gonski³⁹, S. González de la Hoz¹⁷², S. Gonzalez Fernandez¹⁴, R. Gonzalez Lopez⁹⁰, C. Gonzalez Renteria¹⁸, R. Gonzalez Suarez¹⁷⁰, S. Gonzalez-Sevilla⁵⁴, G. R. Gonzalez Rodriguez¹⁷², L. Goossens³⁶, N. A. Gorasia²¹, P. A. Gorbounov¹²³, H. A. Gordon²⁹, B. Gorini³⁶, E. Gorini^{67a,67b}, A. Gorišek⁹¹, A. T. Goshaw⁴⁹, M. I. Gostkin⁷⁹, C. A. Gottardo¹¹⁸, M. Goughri^{35b}, V. Goumarre⁴⁶, A. G. Goussiou¹⁴⁷, N. Govender^{33c}, C. Goy⁵, I. Grabowska-Bold^{83a}, E. Gramstad¹³², S. Grancagnolo¹⁹, M. Grandi¹⁵⁵, V. Gratchev¹³⁶, P. M. Gravila^{27f}, F. G. Gravili^{67a,67b}, H. M. Gray¹⁸, C. Greife²⁴, I. M. Gregor⁴⁶, P. Grenier¹⁵², K. Grevtsov⁴⁶, C. Grieco¹⁴, N. A. Grieser¹²⁷, A. A. Grillo¹⁴⁴, K. Grimm^{31,m}, S. Grinstein^{14,x}, J.-F. Grivaz⁶⁴, S. Groh⁹⁹, E. Gross¹⁷⁸, J. Grosse-Knetter⁵³, Z. J. Grout⁹⁴, C. Grud¹⁰⁵, A. Grummer¹¹⁷, J. C. Grundy¹³³, L. Guan¹⁰⁵, W. Guan¹⁷⁹, C. Gubbels¹⁷³, J. Guenther³⁶, J. G. R. Guerrero Rojas¹⁷², F. Guescini¹¹⁴, D. Guest¹⁹, R. Gugel⁹⁹, A. Guida⁴⁶, T. Guillemin⁵, S. Guindon³⁶, J. Guo^{60c}, L. Guo⁶⁴, Y. Guo¹⁰⁵, R. Gupta⁴⁶, S. Gurbuz²⁴, G. Gustavino¹²⁷, M. Guth⁵², P. Gutierrez¹²⁷, L. F. Gutierrez Zagazeta¹³⁵, C. Gutschow⁹⁴, C. Guyot¹⁴³, C. Gwenlan¹³³, C. B. Gwilliam⁹⁰, E. S. Haaland¹³²

A. Haas¹²⁴, M. H. Habedank¹⁹, C. Haber¹⁸, H. K. Hadavand⁸, A. Hader⁹⁹, M. Haleem¹⁷⁵, J. Haley¹²⁸, J. J. Hall¹⁴⁸, G. Halladjian¹⁰⁶, G. D. Hallewell¹⁰¹, L. Halser²⁰, K. Hamano¹⁷⁴, H. Hamdaoui^{35f}, M. Hamer²⁴, G. N. Hamity⁵⁰, K. Han^{60a}, L. Han^{15c}, L. Han^{60a}, S. Han¹⁸, Y. F. Han¹⁶⁵, K. Hanagaki^{81.v}, M. Hance¹⁴⁴, M. D. Hank³⁷, R. Hankache¹⁰⁰, E. Hansen⁹⁶, J. B. Hansen⁴⁰, J. D. Hansen⁴⁰, M. C. Hansen²⁴, P. H. Hansen⁴⁰, E. C. Hanson¹⁰⁰, K. Hara¹⁶⁷, T. Harenberg¹⁸⁰, S. Harkusha¹⁰⁷, Y. T. Harris¹³³, P. F. Harrison¹⁷⁶, N. M. Hartman¹⁵², N. M. Hartmann¹¹³, Y. Hasegawa¹⁴⁹, A. Hasib⁵⁰, S. Hassani¹⁴³, S. Haug²⁰, R. Hauser¹⁰⁶, M. Havranek¹⁴⁰, C. M. Hawkes²¹, R. J. Hawkins³⁶, S. Hayashida¹¹⁶, D. Hayden¹⁰⁶, C. Hayes¹⁰⁵, R. L. Hayes¹⁷³, C. P. Hays¹³³, J. M. Hays⁹², H. S. Hayward⁹⁰, S. J. Haywood¹⁴², F. He^{60a}, Y. He¹⁶³, Y. He¹³⁴, M. P. Heath⁵⁰, V. Hedberg⁹⁶, A. L. Heggelund¹³², N. D. Hehir⁹², C. Heidegger⁵², K. K. Heidegger⁵², W. D. Heidorn⁷⁸, J. Heilman³⁴, S. Heim⁴⁶, T. Heim¹⁸, B. Heinemann^{46.aj}, J. G. Heinlein¹³⁵, J. J. Heinrich¹³⁰, L. Heinrich³⁶, J. Hejbal¹³⁹, L. Helary⁴⁶, A. Held¹²⁴, S. Hellesund¹³², C. M. Helling¹⁴⁴, S. Hellman^{45a,45b}, C. Helsen³⁶, R. C. W. Henderson⁸⁹, L. Henkelmann³², A. M. Henriques Correia³⁶, H. Herde¹⁵², Y. Hernández Jiménez^{33e}, H. Herr⁹⁹, M. G. Herrmann¹¹³, T. Herrmann⁴⁸, G. Herten⁵², R. Hertenberger¹¹³, L. Hervas³⁶, N. P. Hesse^{166a}, H. Hibi⁸², S. Higashino⁸¹, E. Higón-Rodríguez¹⁷², K. Hildebrand³⁷, K. K. Hill²⁹, K. H. Hiller⁴⁶, S. J. Hillier²¹, M. Hils⁴⁸, I. Hinchliffe¹⁸, F. Hinterkeuser²⁴, M. Hirose¹³¹, S. Hirose¹⁶⁷, D. Hirschbuehl¹⁸⁰, B. Hiti⁹¹, O. Hladik¹³⁹, J. Hobbs¹⁵⁴, R. Hobincu^{27e}, N. Hod¹⁷⁸, M. C. Hodgkinson¹⁴⁸, B. H. Hodgkinson³², A. Hoecker³⁶, J. Hofer⁴⁶, D. Hohn⁵², T. Holm²⁴, T. R. Holmes³⁷, M. Holzbock¹¹⁴, L. B. A. H. Hommels³², B. P. Honan¹⁰⁰, T. M. Hong¹³⁷, J. C. Honig⁵², A. Hönle¹¹⁴, B. H. Hooberman¹⁷¹, W. H. Hopkins⁶, Y. Horii¹¹⁶, P. Horn⁴⁸, L. A. Horyn³⁷, S. Hou¹⁵⁷, J. Howarth⁵⁷, J. Hoya⁸⁸, M. Hrabovsky¹²⁹, A. Hrynevich¹⁰⁸, T. Hryn'ova⁵, P. J. Hsu⁶³, S.-C. Hsu¹⁴⁷, Q. Hu³⁹, S. Hu^{60c}, Y. F. Hu^{15a,15d,an}, D. P. Huang⁹⁴, X. Huang^{15c}, Y. Huang^{60a}, Y. Huang^{15a}, Z. Hubacek¹⁴⁰, F. Hubaut¹⁰¹, M. Huebner²⁴, F. Huegging²⁴, T. B. Huffman¹³³, M. Huhtinen³⁶, R. Hulsken⁵⁸, R. F. H. Hunter³⁴, N. Huseynov^{79.ac}, J. Huston¹⁰⁶, J. Huth⁵⁹, R. Hyneman¹⁵², S. Hyrych^{28a}, G. Iacobucci⁵⁴, G. Iakovidis²⁹, I. Ibragimov¹⁵⁰, L. Iconomidou-Fayard⁶⁴, P. Iengo³⁶, R. Ignazzi⁴⁰, O. Igonkina¹¹⁹, R. Iguchi¹⁶², T. Iizawa⁵⁴, Y. Ikegami⁸¹, N. Ilic^{165,165}, H. Imam^{35a}, G. Introzzi^{70a,70b}, M. Iodice^{74a}, K. Jordanidou^{166a}, V. Ippolito^{72a,72b}, M. Ishino¹⁶², W. Islam¹²⁸, C. Issever^{19,46}, S. Istin^{12c}, J. M. Iturbe Ponce^{62a}, R. Iuppa^{75a,75b}, A. Ivina¹⁷⁸, J. M. Izen⁴³, V. Izzo^{69a}, P. Jacka¹³⁹, P. Jackson¹, R. M. Jacobs⁴⁶, B. P. Jaeger¹⁵¹, C. S. Jagfeld¹¹³, G. Jäkel¹⁸⁰, K. B. Jakobi⁹⁹, K. Jakobs⁵², T. Jakoubek¹⁷⁸, J. Jamieson⁵⁷, K. W. Janas^{83a}, G. Jarlskog⁹⁶, A. E. Jaspán⁹⁰, N. Javadov^{79.ac}, T. Javůrek³⁶, M. Javurkova¹⁰², F. Jeanneau¹⁴³, L. Jeanty¹³⁰, J. Jejelava^{158a}, P. Jenni^{52.e}, S. Jézéquel⁵, J. Jia¹⁵⁴, Z. Jia^{15c}, Y. Jiang^{60a}, S. Jiggins⁵², F. A. Jimenez Morales³⁸, J. Jimenez Pena¹¹⁴, S. Jin^{15c}, A. Jinaru^{27b}, O. Jinnouchi¹⁶³, H. Jivan^{33e}, P. Johansson¹⁴⁸, K. A. Johns⁷, C. A. Johnson⁶⁵, E. Jones¹⁷⁶, R. W. L. Jones⁸⁹, T. J. Jones⁹⁰, J. Jovicevic³⁶, X. Ju¹⁸, J. J. Junggeburth¹¹⁴, A. Juste Rozas^{14.x}, A. Kaczmarska⁸⁴, M. Kado^{72a,72b}, H. Kagan¹²⁶, M. Kagan¹⁵², A. Kahn³⁹, C. Kahra⁹⁹, T. Kaji¹⁷⁷, E. Kajomovitz¹⁵⁹, C. W. Kalderon²⁹, A. Kaluza⁹⁹, A. Kamenshchikov¹²², M. Kaneda¹⁶², N. J. Kang¹⁴⁴, S. Kang⁷⁸, Y. Kano¹¹⁶, J. Kanzaki⁸¹, D. Kar^{33e}, K. Karava¹³³, M. J. Kareem^{166b}, I. Karkanas¹⁶¹, S. N. Karpov⁷⁹, Z. M. Karpova⁷⁹, V. Kartvelishvili⁸⁹, A. N. Karyukhin¹²², E. Kasimi¹⁶¹, C. Kato^{60d}, J. Katzy⁴⁶, K. Kawade¹⁴⁹, K. Kawagoe⁸⁷, T. Kawaguchi¹¹⁶, T. Kawamoto¹⁴³, G. Kawamura⁵³, E. F. Kay¹⁷⁴, F. I. Kaya¹⁶⁸, S. Kazakos¹⁴, V. F. Kazanin^{121a,121b}, Y. Ke¹⁵⁴, J. M. Keaveney^{33a}, R. Keeler¹⁷⁴, J. S. Keller³⁴, D. Kelsey¹⁵⁵, J. J. Kempster²¹, J. Kendrick²¹, K. E. Kennedy³⁹, O. Kepka¹³⁹, S. Kersten¹⁸⁰, B. P. Kerševan⁹¹, S. Ketabchi Haghighat¹⁶⁵, F. Khalil-Zada¹³, M. Khandoga¹³⁴, A. Khanov¹²⁸, A. G. Kharlamov^{121a,121b}, T. Kharlamova^{121a,121b}, E. E. Khoda¹⁷³, T. J. Khoo¹⁹, G. Khorauli¹⁷⁵, E. Khramov⁷⁹, J. Khubua^{158b}, S. Kido⁸², M. Kiehn³⁶, A. Kilgallon¹³⁰, E. Kim¹⁶³, Y. K. Kim³⁷, N. Kimura⁹⁴, A. Kirchhoff⁵³, D. Kirchmeier⁴⁸, J. Kirk¹⁴², A. E. Kiryunin¹¹⁴, T. Kishimoto¹⁶², D. P. Kisluk¹⁶⁵, V. Kitali⁴⁶, C. Kitsaki¹⁰, O. Kivernykh²⁴, T. Klapdor-Kleingrothaus⁵², M. Klassen^{61a}, C. Klein³⁴, L. Klein¹⁷⁵, M. H. Klein¹⁰⁵, M. Klein⁹⁰, U. Klein⁹⁰, P. Klimek³⁶, A. Klimentov²⁹, F. Klimpel³⁶, T. Klingl²⁴, T. Klioutchnikova³⁶, F. F. Klitzner¹¹³, P. Kluit¹¹⁹, S. Kluth¹¹⁴, E. Kneringer⁷⁶, T. M. Knight¹⁶⁵, A. Knue⁵², D. Kobayashi⁸⁷, M. Kobel⁴⁸, M. Kocian¹⁵², T. Kodama¹⁶², P. Kodys¹⁴¹, D. M. Koeck¹⁵⁵, P. T. Koenig²⁴, T. Koffas³⁴, N. M. Köhler³⁶, M. Kolb¹⁴³, I. Koletsou⁵, T. Komarek¹²⁹, K. Köneke⁵², A. X. Y. Kong¹, T. Kono¹²⁵, V. Konstantinides⁹⁴, N. Konstantinidis⁹⁴, B. Konya⁹⁶, R. Kopeliansky⁶⁵, S. Koperny^{83a}, K. Korcyl⁸⁴, K. Kordas¹⁶¹, G. Koren¹⁶⁰, A. Korn⁹⁴, S. Korn⁵³, I. Korolkov¹⁴, E. V. Korolkova¹⁴⁸, N. Korotkova¹¹², O. Kortner¹¹⁴, S. Kortner¹¹⁴, V. V. Kostyukhin^{148,164}, A. Kotskechagia⁶⁴, A. Kotwal⁴⁹, A. Koulouris⁹, A. Kourkoumeli-Charalampidi^{70a,70b}, C. Kourkoumelis⁹, E. Kourlitis⁶, R. Kowalewski¹⁷⁴, W. Kozanecki¹⁴³, A. S. Kozhin¹²², V. A. Kramarenko¹¹², G. Kramberger⁹¹

D. Krasnopevtsev^{60a}, M. W. Krasny¹³⁴, A. Krasznahorkay³⁶, J. A. Kremer⁹⁹, J. Kretzschmar⁹⁰, K. Kreul¹⁹, P. Krieger¹⁶⁵, F. Krieter¹¹³, S. Krishnamurthy¹⁰², A. Krishnan^{61b}, M. Krivos¹⁴¹, K. Krizka¹⁸, K. Kroeninger⁴⁷, H. Kroha¹¹⁴, J. Kroll¹³⁹, J. Kroll¹³⁵, K. S. Krowpman¹⁰⁶, U. Kruchonak⁷⁹, H. Krüger²⁴, N. Krumnack⁷⁸, M. C. Kruse⁴⁹, J. A. Krzysiak⁸⁴, A. Kubota¹⁶³, O. Kuchinskaja¹⁶⁴, S. Kuday^{4b}, D. Kuechler⁴⁶, J. T. Kuechler⁴⁶, S. Kuehn³⁶, T. Kuhl⁴⁶, V. Kukhtin⁷⁹, Y. Kulchitsky^{107.af}, S. Kuleshov^{145b}, M. Kumar^{33e}, N. Kumari¹⁰¹, M. Kuna⁵⁸, A. Kupco¹³⁹, T. Kupfer⁴⁷, O. Kuprash⁵², H. Kurashige⁸², L. L. Kurchaninov^{166a}, Y. A. Kurochkin¹⁰⁷, A. Kurova¹¹¹, M. G. Kurth^{15a,15d}, E. S. Kuwertz³⁶, M. Kuze¹⁶³, A. K. Kvam¹⁴⁷, J. Kvita¹²⁹, T. Kwan¹⁰³, C. Lacasta¹⁷², F. Lacava^{72a,72b}, D. P. J. Lack¹⁰⁰, H. Lacker¹⁹, D. Lacour¹³⁴, E. Ladygin⁷⁹, R. Lafaye⁵, B. Laforge¹³⁴, T. Lagouri^{145c}, S. Lai⁵³, I. K. Lakomic^{83a}, N. Lalloue⁵⁸, J. E. Lambert¹²⁷, S. Lammers⁶⁵, W. Lampf⁷, C. Lampoudis¹⁶¹, E. Lançon²⁹, U. Landgraf⁵², M. P. J. Landon⁹², V. S. Lang⁵², J. C. Lange⁵³, R. J. Langenberg¹⁰², A. J. Lankford¹⁶⁹, F. Lanni²⁹, K. Lantzsch²⁴, A. Lanza^{70a}, A. Lapertosa^{55b,55a}, J. F. Laporte¹⁴³, T. Lari^{68a}, F. Lasagni Manghi^{23a,23b}, M. Lassnig³⁶, V. Latonova¹³⁹, T. S. Lau^{62a}, A. Laudrain⁹⁹, A. Laurier³⁴, M. Lavorgna^{69a,69b}, S. D. Lawlor⁹³, M. Lazzaroni^{68a,68b}, B. Le¹⁰⁰, A. Lebedev⁷⁸, M. LeBlanc⁷, T. LeCompte⁶, F. Ledroit-Guillon⁵⁸, A. C. A. Lee⁹⁴, C. A. Lee²⁹, G. R. Lee¹⁷, L. Lee⁵⁹, S. C. Lee¹⁵⁷, S. Lee⁷⁸, L. L. Leeuw^{33c}, B. Lefebvre^{166a}, H. P. Lefebvre⁹³, M. Lefebvre¹⁷⁴, C. Leggett¹⁸, K. Lehmann¹⁵¹, N. Lehmann²⁰, G. Lehmann Miotto³⁶, W. A. Leight⁴⁶, A. Leisos^{161.w}, M. A. L. Leite^{80c}, C. E. Leitgeb¹¹³, R. Leitner¹⁴¹, K. J. C. Leney⁴², T. Lenz²⁴, S. Leone^{71a}, C. Leonidopoulos⁵⁰, A. Leopold¹³⁴, C. Leroy¹⁰⁹, R. Les¹⁰⁶, C. G. Lester³², M. Levchenko¹³⁶, J. Levêque⁵, D. Levin¹⁰⁵, L. J. Levinson¹⁷⁸, D. J. Lewis²¹, B. Li^{15b}, B. Li¹⁰⁵, C. Q. Li^{60c,60d}, F. Li^{60c}, H. Li^{60a}, H. Li^{60b}, J. Li^{60c}, K. Li¹⁴⁷, L. Li^{60c}, M. Li^{15a,15d}, Q. Y. Li^{60a}, S. Li^{60d,60c,c}, X. Li⁴⁶, Y. Li⁴⁶, Z. Li^{60b}, Z. Li¹³³, Z. Li¹⁰³, Z. Li⁹⁰, Z. Liang^{15a}, M. Liberatore⁴⁶, B. Liberti^{73a}, K. Lie^{62c}, C. Y. Lin³², K. Lin¹⁰⁶, R. A. Linck⁶⁵, R. E. Lindley⁷, J. H. Lindon²¹, A. Lins⁴⁶, A. L. Lioni⁵⁴, E. Lipeles¹³⁵, A. Lipniacka¹⁷, T. M. Liss^{171.ak}, A. Lister¹⁷³, J. D. Little⁸, B. Liu^{15a}, B. X. Liu¹⁵¹, J. B. Liu^{60a}, J. K. K. Liu³⁷, K. Liu^{60d,60c}, M. Liu^{60a}, M. Y. Liu^{60a}, P. Liu^{15a}, X. Liu^{60a}, Y. Liu⁴⁶, Y. Liu^{15a,15d}, Y. L. Liu¹⁰⁵, Y. W. Liu^{60a}, M. Livan^{70a,70b}, A. Lleres⁵⁸, J. Llorente Merino¹⁵¹, S. L. Lloyd⁹², E. M. Lobodzinska⁴⁶, P. Loch⁷, S. Loffredo^{73a,73b}, T. Lohse¹⁹, K. Lohwasser¹⁴⁸, M. Lokajicek¹³⁹, J. D. Long¹⁷¹, R. E. Long⁸⁹, I. Longarini^{72a,72b}, L. Longo³⁶, R. Longo¹⁷¹, I. Lopez Paz¹⁴, A. Lopez Solis⁴⁶, J. Lorenz¹¹³, N. Lorenzo Martinez⁵, A. M. Lory¹¹³, A. Lösle⁵², X. Lou^{45a,45b}, X. Lou^{15a}, A. Lounis⁶⁴, J. Love⁶, P. A. Love⁸⁹, J. J. Lozano Bahilo¹⁷², G. Lu^{15a}, M. Lu^{60a}, S. Lu¹³⁵, Y. J. Lu⁶³, H. J. Lubatti¹⁴⁷, C. Luci^{72a,72b}, F. L. Lucio Alves^{15c}, A. Lucotte⁵⁸, F. Luehring⁶⁵, I. Luise¹⁵⁴, L. Luminari^{72a}, B. Lund-Jensen¹⁵³, N. A. Luongo¹³⁰, M. S. Lutz¹⁶⁰, D. Lynn²⁹, H. Lyons⁹⁰, R. Lysak¹³⁹, E. Lytken⁹⁶, F. Lyu^{15a}, V. Lyubushkin⁷⁹, T. Lyubushkina⁷⁹, H. Ma²⁹, L. L. Ma^{60b}, Y. Ma⁹⁴, D. M. Mac Donell¹⁷⁴, G. Maccarrone⁵¹, C. M. Macdonald¹⁴⁸, J. C. MacDonald¹⁴⁸, R. Madar³⁸, W. F. Mader⁴⁸, M. Madugoda Ralalage Don¹²⁸, N. Madysa⁴⁸, J. Maeda⁸², T. Maeno²⁹, M. Maerker⁴⁸, V. Magerl⁵², J. Magro^{66a,66c}, D. J. Mahon³⁹, C. Maidantchik^{80b}, A. Maio^{138a,138b,138d}, K. Maj^{83a}, O. Majersky^{28a}, S. Majewski¹³⁰, N. Makovec⁶⁴, B. Malaescu¹³⁴, Pa. Malecki⁸⁴, V. P. Maleev¹³⁶, F. Malek⁵⁸, D. Malito^{41b,41a}, U. Mallik⁷⁷, C. Malone³², S. Maltezos¹⁰, S. Malyukov⁷⁹, J. Mamuzic¹⁷², G. Mancini⁵¹, J. P. Mandalia⁹², I. Mandić⁹¹, L. Manhaes de Andrade Filho^{80a}, I. M. Maniatis¹⁶¹, M. Manisha¹⁴³, J. Manjarres Ramos⁴⁸, K. H. Mankinen⁹⁶, A. Mann¹¹³, A. Manousos⁷⁶, B. Mansoulié¹⁴³, I. Manthos¹⁶¹, S. Manzoni¹¹⁹, A. Marantis¹⁶¹, L. Marchese¹³³, G. Marchiori¹³⁴, M. Marcisovsky¹³⁹, L. Marcocchia^{73a,73b}, C. Marcon⁹⁶, M. Marjanovic¹²⁷, Z. Marshall¹⁸, S. Marti-Garcia¹⁷², T. A. Martin¹⁷⁶, V. J. Martin⁵⁰, B. Martin dit Latour¹⁷, L. Martinelli^{74a,74b}, M. Martinez^{14.x}, P. Martinez Agullo¹⁷², V. I. Martinez Outschoorn¹⁰², S. Martin-Haugh¹⁴², V. S. Martoiu^{27b}, A. C. Martyniuk⁹⁴, A. Marzin³⁶, S. R. Maschek¹¹⁴, L. Masetti⁹⁹, T. Mashimo¹⁶², R. Mashinistov¹¹⁰, J. Masik¹⁰⁰, A. L. Maslennikov^{121a,121b}, L. Massa^{23a,23b}, P. Massarotti^{69a,69b}, P. Mastrandrea^{71a,71b}, A. Mastroberardino^{41b,41a}, T. Masubuchi¹⁶², D. Matakias²⁹, T. Mathisen¹⁷⁰, A. Matic¹¹³, N. Matsuzawa¹⁶², J. Maurer^{27b}, B. Maček⁹¹, D. A. Maximov^{121a,121b}, R. Mazini¹⁵⁷, I. Maznas¹⁶¹, S. M. Mazza¹⁴⁴, C. Mc Ginn²⁹, J. P. Mc Gowan¹⁰³, S. P. Mc Kee¹⁰⁵, T. G. McCarthy¹¹⁴, W. P. McCormack¹⁸, E. F. McDonald¹⁰⁴, A. E. McDougall¹¹⁹, J. A. Mcfayden¹⁵⁵, G. Mchedlidze^{158b}, M. A. McKay⁴², K. D. McLean¹⁷⁴, S. J. McMahon¹⁴², P. C. McNamara¹⁰⁴, R. A. McPherson^{174.ab}, J. E. Mdhuli^{33e}, Z. A. Meadows¹⁰², S. Meehan³⁶, T. Megy³⁸, S. Mehlhase¹¹³, A. Mehta⁹⁰, B. Meirose⁴³, D. Melini¹⁵⁹, B. R. Mellado Garcia^{33e}, F. Meloni⁴⁶, A. Melzer²⁴, E. D. Mendes Gouveia^{138a,138e}, A. M. Mendes Jacques Da Costa²¹, H. Y. Meng¹⁶⁵, L. Meng³⁶, S. Menke¹¹⁴, E. Meoni^{41b,41a}, S. A. M. Merkt¹³⁷, C. Merlassino¹³³, P. Mermod⁵⁴, L. Merola^{69a,69b}

D. Pohl²⁴, I. Pokharel⁵³, G. Polesello^{70a}, A. Poley^{151,166a}, A. Policicchio^{72a,72b}, R. Polifka¹⁴¹, A. Polini^{23b}, C. S. Pollard⁴⁶, Z. B. Pollock¹²⁶, V. Polychronakos²⁹, D. Ponomarenko¹¹¹, L. Pontecorvo³⁶, S. Popa^{27a}, G. A. Popeneciu^{27d}, L. Portales⁵, D. M. Portillo Quintero⁵⁸, S. Pospisil¹⁴⁰, P. Postolache^{27c}, K. Potamianos¹³³, I. N. Potrap⁷⁹, C. J. Potter³², H. Potti¹¹, T. Poulsen⁴⁶, J. Poveda¹⁷², T. D. Powell¹⁴⁸, G. Pownall⁴⁶, M. E. Pozo Astigarraga³⁶, A. Prades Ibanez¹⁷², P. Pralavorio¹⁰¹, M. M. Prapa⁴⁴, S. Prell⁷⁸, D. Price¹⁰⁰, M. Primavera^{67a}, M. L. Proffitt¹⁴⁷, N. Proklova¹¹¹, K. Prokofiev^{62c}, F. Prokoshin⁷⁹, S. Protopopescu²⁹, J. Proudfoot⁶, M. Przybycien^{83a}, D. Pudzha¹³⁶, P. Puzo⁶⁴, D. Pyatiizbyantseva¹¹¹, J. Qian¹⁰⁵, Y. Qin¹⁰⁰, A. Quadt⁵³, M. Queitsch-Maitland³⁶, G. Rabanal Bolanos⁵⁹, F. Ragusa^{68a,68b}, G. Rahal⁹⁷, J. A. Raine⁵⁴, S. Rajagopalan²⁹, K. Ran^{15a,15d}, D. F. Rassloff^{61a}, D. M. Rauch⁴⁶, S. Rave⁹⁹, B. Ravina⁵⁷, I. Ravinovitch¹⁷⁸, M. Raymond³⁶, A. L. Read¹³², N. P. Readioff¹⁴⁸, M. Reale^{67a,67b}, D. M. Rebuffi^{70a,70b}, G. Redlinger²⁹, K. Reeves⁴³, D. Reikher¹⁶⁰, A. Reiss⁹⁹, A. Rej¹⁵⁰, C. Rembser³⁶, A. Renardi⁴⁶, M. Renda^{27b}, M. B. Rendel¹¹⁴, A. G. Rennie⁵⁷, S. Resconi^{68a}, E. D. Resseguie¹⁸, S. Rettie⁹⁴, B. Reynolds¹²⁶, E. Reynolds²¹, M. Rezaei Estabragh¹⁸⁰, O. L. Rezanova^{121a,121b}, P. Reznicek¹⁴¹, E. Ricci^{75a,75b}, R. Richter¹¹⁴, S. Richter⁴⁶, E. Richter-Was^{83b}, M. Ridel¹³⁴, P. Rieck¹¹⁴, O. Rifki⁴⁶, M. Rijssenbeek¹⁵⁴, A. Rimoldi^{70a,70b}, M. Rimoldi⁴⁶, L. Rinaldi^{23b}, T. T. Rinn¹⁷¹, M. P. Rinnagel¹¹³, G. Ripellino¹⁵³, I. Riu¹⁴, P. Rivadeneira⁴⁶, J. C. Rivera Vergara¹⁷⁴, F. Rizatdinova¹²⁸, E. Rizvi⁹², C. Rizzi⁵⁴, S. H. Robertson^{103.ab}, M. Robin⁴⁶, D. Robinson³², C. M. Robles Gajardo^{145d}, M. Robles Manzano⁹⁹, A. Robson⁵⁷, A. Rocchi^{73a,73b}, C. Roda^{71a,71b}, S. Rodriguez Bosca¹⁷², A. Rodriguez Rodriguez⁵², A. M. Rodríguez Vera^{166b}, S. Roe³⁶, J. Roggel¹⁸⁰, O. Røhne¹³², R. A. Rojas^{145d}, B. Roland⁵², C. P. A. Roland⁶⁵, J. Roloff²⁹, A. Romaniouk¹¹¹, M. Romano^{23a,23b}, N. Rompotis⁹⁰, M. Ronzani¹²⁴, L. Roos¹³⁴, S. Rosati^{72a}, G. Rosin¹⁰², B. J. Rosser¹³⁵, E. Rossi¹⁶⁵, E. Rossi⁵, E. Rossi^{69a,69b}, L. P. Rossi^{55b}, L. Rossini⁴⁶, R. Rosten¹²⁶, M. Rotaru^{27b}, B. Rottler⁵², D. Rousseau⁶⁴, D. Rouso³², G. Rovelli^{70a,70b}, A. Roy¹¹, A. Rozanov¹⁰¹, Y. Rozen¹⁵⁹, X. Ruan^{33e}, A. J. Ruby⁹⁰, T. A. Ruggeri¹, F. Rühr⁵², A. Ruiz-Martinez¹⁷², A. Rummler³⁶, Z. Rurikova⁵², N. A. Rusakovich⁷⁹, H. L. Russell³⁶, L. Rustige³⁸, J. P. Rutherford⁷, E. M. Rüttinger¹⁴⁸, M. Rybar¹⁴¹, E. B. Rye¹³², A. Ryzhov¹²², J. A. Sabater Iglesias⁴⁶, P. Sabatini¹⁷², L. Sabetta^{72a,72b}, H.F.-W. Sadrozinski¹⁴⁴, R. Sadykov⁷⁹, F. Safai Tehrani^{72a}, B. Safarzadeh Samani¹⁵⁵, M. Safdari¹⁵², P. Saha¹²⁰, S. Saha¹⁰³, M. Sahinsoy¹¹⁴, A. Sahu¹⁸⁰, M. Saimpert³⁶, M. Saito¹⁶², T. Saito¹⁶², D. Salamani⁵⁴, G. Salamanna^{74a,74b}, A. Salmikov¹⁵², J. Salt¹⁷², A. Salvador Salas¹⁴, D. Salvatore^{41b,41a}, F. Salvatore¹⁵⁵, A. Salzburger³⁶, D. Sammel⁵², D. Sampsonidis¹⁶¹, D. Sampsonidou^{60d,60c}, J. Sánchez¹⁷², A. Sanchez Pineda^{66a,36,66c}, H. Sandaker¹³², C. O. Sander⁴⁶, I. G. Sanderswood⁸⁹, M. Sandhoff¹⁸⁰, C. Sandoval^{22b}, D. P. C. Sankey¹⁴², M. Sannino^{55b,55a}, Y. Sano¹¹⁶, A. Sansoni⁵¹, C. Santoni³⁸, H. Santos^{138a,138b}, S. N. Santpur¹⁸, A. Santra¹⁷⁸, K. A. Saoucha¹⁴⁸, A. Sapronov⁷⁹, J. G. Saraiva^{138a,138d}, O. Sasaki⁸¹, K. Sato¹⁶⁷, C. Sauer^{61b}, F. Sauerburger⁵², E. Sauvan⁵, P. Savard^{165.al}, R. Sawada¹⁶², C. Sawyer¹⁴², L. Sawyer⁹⁵, I. Sayago Galvan¹⁷², C. Sbarra^{23b}, A. Sbrizzi^{66a,66c}, T. Scanlon⁹⁴, J. Schaarschmidt¹⁴⁷, P. Schacht¹¹⁴, D. Schaefer³⁷, L. Schaefer¹³⁵, U. Schäfer⁹⁹, A. C. Schaffer⁶⁴, D. Schaile¹¹³, R. D. Schamberger¹⁵⁴, E. Schanet¹¹³, C. Scharf¹⁹, N. Scharmberg¹⁰⁰, V. A. Schegelsky¹³⁶, D. Scheirich¹⁴¹, F. Schenck¹⁹, M. Schernau¹⁶⁹, C. Schiavi^{55b,55a}, L. K. Schildgen²⁴, Z. M. Schillaci²⁶, E. J. Schioppa^{67a,67b}, M. Schioppa^{41b,41a}, B. Schlag⁹⁹, K. E. Schleicher⁵², S. Schlenker³⁶, K. Schmieden⁹⁹, C. Schmitt⁹⁹, S. Schmitt⁴⁶, L. Schoeffel¹⁴³, A. Schoening^{61b}, P. G. Scholer⁵², E. Schopf¹³³, M. Schott⁹⁹, J. Schovancova³⁶, S. Schramm⁵⁴, F. Schroeder¹⁸⁰, A. Schulte⁹⁹, H.-C. Schultz-Coulon^{61a}, M. Schumacher⁵², B. A. Schumm¹⁴⁴, Ph. Schune¹⁴³, A. Schwartzman¹⁵², T. A. Schwarz¹⁰⁵, Ph. Schwemling¹⁴³, R. Schwienhorst¹⁰⁶, A. Sciandra¹⁴⁴, G. Sciolla²⁶, F. Scuri^{71a}, F. Scutti¹⁰⁴, C. D. Sebastiani⁹⁰, K. Sedlaczek⁴⁷, P. Seema¹⁹, S. C. Seidel¹¹⁷, A. Seiden¹⁴⁴, B. D. Seidlitz²⁹, T. Seiss³⁷, C. Seitz⁴⁶, J. M. Seixas^{80b}, G. Sekhniaidze^{69a}, S. J. Sekula⁴², L. P. Selem⁵, N. Semprini-Cesari^{23a,23b}, S. Sen⁴⁹, C. Serfon²⁹, L. Serin⁶⁴, L. Serkin^{66a,66b}, M. Sessa^{60a}, H. Severini¹²⁷, S. Sevova¹⁵², F. Sforza^{55b,55a}, A. Sfyrila⁵⁴, E. Shabalina⁵³, J. D. Shahinian¹³⁵, N. W. Shaikh^{45a,45b}, D. Shaked Renous¹⁷⁸, L. Y. Shan^{15a}, M. Shapiro¹⁸, A. Sharma³⁶, A. S. Sharma¹, S. Sharma⁴⁶, P. B. Shatalov¹²³, K. Shaw¹⁵⁵, S. M. Shaw¹⁰⁰, M. Shehade¹⁷⁸, Y. Shen¹²⁷, N. Sherafati³⁴, P. Sherwood⁹⁴, L. Shi⁹⁴, C. O. Shimmin¹⁸¹, Y. Shimogama¹⁷⁷, M. Shimogima¹¹⁵, J. D. Shinner⁹³, I. P. J. Shipsey¹³³, S. Shirabe¹⁶³, M. Shiyakova^{79,z}, J. Shlomi¹⁷⁸, M. J. Shochet³⁷, J. Shojaii¹⁰⁴, D. R. Shope¹⁵³, S. Shrestha¹²⁶, E. M. Shrif^{33e}, M. J. Shroff¹⁷⁴, E. Shulga¹⁷⁸, P. Sicho¹³⁹, A. M. Sickles¹⁷¹, E. Sideras Haddad^{33e}, O. Sidiropoulou³⁶, A. Sidoti^{23a,23b}, F. Siegert⁴⁸, Dj. Sijacki¹⁶, M. V. Silva Oliveira³⁶, S. B. Silverstein^{45a}, S. Simion⁶⁴, E. Simioni⁹⁹, R. Simoniello³⁶, S. Simsek^{12b}, P. Sinervo¹⁶⁵, V. Sinetckii¹¹², S. Singh¹⁵¹, S. Sinha^{33e}, M. Sioli^{23a,23b}, I. Siral¹³⁰, S. Yu. Sivoklokov¹¹², J. Sjölín^{45a,45b}, A. Skaf⁵³, E. Skorda⁹⁶

N. K. Vu¹⁰¹, R. Vuillermet³⁶, I. Vukotic³⁷, S. Wada¹⁶⁷, C. Wagner¹⁰², P. Wagner²⁴, W. Wagner¹⁸⁰, S. Wahdan¹⁸⁰, H. Wahlberg⁸⁸, R. Wakasa¹⁶⁷, M. Wakida¹¹⁶, V. M. Walbrecht¹¹⁴, J. Walder¹⁴², R. Walker¹¹³, S. D. Walker⁹³, W. Walkowiak¹⁵⁰, V. Wallangen^{45a,45b}, A. M. Wang⁵⁹, A. Z. Wang¹⁷⁹, C. Wang^{60a}, C. Wang^{60c}, H. Wang¹⁸, J. Wang^{62a}, P. Wang⁴², R.-J. Wang⁹⁹, R. Wang⁵⁹, R. Wang¹²⁰, S. M. Wang¹⁵⁷, S. Wang^{60b}, T. Wang^{60a}, W. T. Wang^{60a}, W. X. Wang^{60a}, X. Wang¹⁷¹, Y. Wang^{60a}, Z. Wang¹⁰⁵, C. Wanotayaroj³⁶, A. Warburton¹⁰³, C. P. Ward³², R. J. Ward²¹, N. Warrack⁵⁷, A. T. Watson²¹, M. F. Watson²¹, G. Watts¹⁴⁷, B. M. Waugh⁹⁴, A. F. Webb¹¹, C. Weber²⁹, M. S. Weber²⁰, S. A. Weber³⁴, S. M. Weber^{61a}, C. Wei^{60a}, Y. Wei¹³³, A. R. Weidberg¹³³, J. Weingarten⁴⁷, M. Weirich⁹⁹, C. Weiser⁵², P. S. Wells³⁶, T. Wenaus²⁹, B. Wendland⁴⁷, T. Wengler³⁶, S. Wenig³⁶, N. Vermes²⁴, M. Wessels^{61a}, T. D. Weston²⁰, K. Whalen¹³⁰, A. M. Wharton⁸⁹, A. S. White⁵⁹, A. White⁸, M. J. White¹, D. Whiteson¹⁶⁹, W. Wiedenmann¹⁷⁹, C. Wiel⁴⁸, M. Wielers¹⁴², N. Wieseotte⁹⁹, C. Wiglesworth⁴⁰, L. A. M. Wiik-Fuchs⁵², H. G. Wilkens³⁶, L. J. Wilkins⁹³, D. M. Williams³⁹, H. H. Williams¹³⁵, S. Williams³², S. Willocq¹⁰², P. J. Windischhofer¹³³, I. Wingerter-Seez⁵, F. Winklmeier¹³⁰, B. T. Winter⁵², M. Wittgen¹⁵², M. Wobisch⁹⁵, A. Wolf⁹⁹, R. Wölker¹³³, J. Wollrath⁵², M. W. Wolter⁸⁴, H. Wolters^{138a,138c}, V. W. S. Wong¹⁷³, A. F. Wongel⁴⁶, N. L. Woods¹⁴⁴, S. D. Worm⁴⁶, B. K. Wosiek⁸⁴, K. W. Woźniak⁸⁴, K. Wraight⁵⁷, J. Wu^{15a,15d}, S. L. Wu¹⁷⁹, X. Wu⁵⁴, Y. Wu^{60a}, Z. Wu¹⁴³, J. Wuerzinger¹³³, T. R. Wyatt¹⁰⁰, B. M. Wynne⁵⁰, S. Xella⁴⁰, J. Xiang^{62c}, X. Xiao¹⁰⁵, X. Xie^{60a}, I. Xiotidis¹⁵⁵, D. Xu^{15a}, H. Xu^{60a}, H. Xu^{60a}, L. Xu^{60a}, R. Xu¹³⁵, W. Xu¹⁰⁵, Y. Xu^{15b}, Z. Xu^{60b}, Z. Xu¹⁵², B. Yabsley¹⁵⁶, S. Yacoub^{33a}, D. P. Yallup⁹⁴, N. Yamaguchi⁸⁷, Y. Yamaguchi¹⁶³, M. Yamatani¹⁶², H. Yamauchi¹⁶⁷, T. Yamazaki¹⁸, Y. Yamazaki⁸², J. Yan^{60c}, Z. Yan²⁵, H. J. Yang^{60c,60d}, H. T. Yang¹⁸, S. Yang^{60a}, T. Yang^{62c}, X. Yang^{60a}, X. Yang^{15a}, Y. Yang¹⁶², Z. Yang^{105,60a}, W.-M. Yao¹⁸, Y. C. Yap⁴⁶, H. Ye^{15c}, J. Ye⁴², S. Ye²⁹, I. Yeletsikh⁷⁹, M. R. Yexley⁸⁹, P. Yin³⁹, K. Yorita¹⁷⁷, K. Yoshihara⁷⁸, C. J. S. Young³⁶, C. Young¹⁵², R. Yuan^{60b,j}, X. Yue^{61a}, M. Zaazoua^{35f}, B. Zabinski⁸⁴, G. Zacharis¹⁰, E. Zaffaroni⁵⁴, J. Zahreddine¹⁰¹, A. M. Zaitsev^{122,ag}, T. Zakareishvili^{158b}, N. Zakharchuk³⁴, S. Zambito³⁶, D. Zanzi⁵², S. V. Zeißner⁴⁷, C. Zeitnitz¹⁸⁰, G. Zemaityte¹³³, J. C. Zeng¹⁷¹, O. Zenin¹²², T. Ženiš^{28a}, S. Zenz⁹², S. Zerradi^{35a}, D. Zerwas⁶⁴, M. Zgubič¹³³, B. Zhang^{15c}, D. F. Zhang^{15b}, G. Zhang^{15b}, J. Zhang⁶, K. Zhang^{15a}, L. Zhang^{15c}, M. Zhang¹⁷¹, R. Zhang¹⁷⁹, S. Zhang¹⁰⁵, X. Zhang^{60c}, X. Zhang^{60b}, Z. Zhang⁶⁴, P. Zhao⁴⁹, Y. Zhao¹⁴⁴, Z. Zhao^{60a}, A. Zhemchugov⁷⁹, Z. Zheng¹⁰⁵, D. Zhong¹⁷¹, B. Zhou¹⁰⁵, C. Zhou¹⁷⁹, H. Zhou⁷, M. Zhou¹⁵⁴, N. Zhou^{60c}, Y. Zhou⁷, C. G. Zhu^{60b}, C. Zhu^{15a,15d}, H. L. Zhu^{60a}, H. Zhu^{15a}, J. Zhu¹⁰⁵, Y. Zhu^{60a}, X. Zhuang^{15a}, K. Zhukov¹¹⁰, V. Zhulanov^{121a,121b}, D. Zieminska⁶⁵, N. I. Zimine⁷⁹, S. Zimmermann^{52,*}, Z. Zinonos¹¹⁴, M. Ziolkowski¹⁵⁰, L. Živković¹⁶, A. Zoccoli^{23a,23b}, K. Zoch⁵³, T. G. Zorbas¹⁴⁸, R. Zou³⁷, W. Zou³⁹, L. Zwalinski³⁶

¹ Department of Physics, University of Adelaide, Adelaide, Australia

² Physics Department, SUNY Albany, Albany, NY, USA

³ Department of Physics, University of Alberta, Edmonton, AB, Canada

⁴ (a) Department of Physics, Ankara University, Ankara, Turkey; (b) Application and Research Center for Advanced Studies, Istanbul Aydin University, Istanbul, Turkey; (c) Division of Physics, TOBB University of Economics and Technology, Ankara, Turkey

⁵ LAPP, Université Grenoble Alpes, Université Savoie Mont Blanc, CNRS/IN2P3, Annecy, France

⁶ High Energy Physics Division, Argonne National Laboratory, Argonne, IL, USA

⁷ Department of Physics, University of Arizona, Tucson, AZ, USA

⁸ Department of Physics, University of Texas at Arlington, Arlington, TX, USA

⁹ Physics Department, National and Kapodistrian University of Athens, Athens, Greece

¹⁰ Physics Department, National Technical University of Athens, Zografou, Greece

¹¹ Department of Physics, University of Texas at Austin, Austin, TX, USA

¹² (a) Bahcesehir University, Faculty of Engineering and Natural Sciences, Istanbul, Turkey; (b) Faculty of Engineering and Natural Sciences, Istanbul Bilgi University, Istanbul, Turkey; (c) Department of Physics, Bogazici University, Istanbul, Turkey; (d) Department of Physics Engineering, Gaziantep University, Gaziantep, Turkey

¹³ Institute of Physics, Azerbaijan Academy of Sciences, Baku, Azerbaijan

¹⁴ Institut de Física d'Altes Energies (IFAE), Barcelona Institute of Science and Technology, Barcelona, Spain

¹⁵ (a) Institute of High Energy Physics, Chinese Academy of Sciences, Beijing, China; (b) Physics Department, Tsinghua University, Beijing, China; (c) Department of Physics, Nanjing University, Nanjing, China; (d) University of Chinese Academy of Science (UCAS), Beijing, China

- ¹⁶ Institute of Physics, University of Belgrade, Belgrade, Serbia
- ¹⁷ Department for Physics and Technology, University of Bergen, Bergen, Norway
- ¹⁸ Physics Division, Lawrence Berkeley National Laboratory and University of California, Berkeley, CA, USA
- ¹⁹ Institut für Physik, Humboldt Universität zu Berlin, Berlin, Germany
- ²⁰ Albert Einstein Center for Fundamental Physics and Laboratory for High Energy Physics, University of Bern, Bern, Switzerland
- ²¹ School of Physics and Astronomy, University of Birmingham, Birmingham, UK
- ²² ^(a)Facultad de Ciencias y Centro de Investigaciones, Universidad Antonio Nariño, Bogotá, Colombia; ^(b)Departamento de Física, Universidad Nacional de Colombia, Bogotá, Colombia, Colombia
- ²³ ^(a)Dipartimento di Fisica, INFN Bologna and Università di Bologna, Bologna, Italy; ^(b)INFN Sezione di Bologna, Bologna, Italy
- ²⁴ Physikalisches Institut, Universität Bonn, Bonn, Germany
- ²⁵ Department of Physics, Boston University, Boston, MA, USA
- ²⁶ Department of Physics, Brandeis University, Waltham, MA, USA
- ²⁷ ^(a)Transilvania University of Brasov, Brasov, Romania; ^(b)Horia Hulubei National Institute of Physics and Nuclear Engineering, Bucharest, Romania; ^(c)Department of Physics, Alexandru Ioan Cuza University of Iasi, Iasi, Romania; ^(d)National Institute for Research and Development of Isotopic and Molecular Technologies, Physics Department, Cluj-Napoca, Romania; ^(e)University Politehnica Bucharest, Bucharest, Romania; ^(f)West University in Timisoara, Timisoara, Romania
- ²⁸ ^(a)Faculty of Mathematics, Physics and Informatics, Comenius University, Bratislava, Slovakia; ^(b)Department of Subnuclear Physics, Institute of Experimental Physics of the Slovak Academy of Sciences, Kosice, Slovak Republic
- ²⁹ Physics Department, Brookhaven National Laboratory, Upton, NY, USA
- ³⁰ Departamento de Física, Universidad de Buenos Aires, Buenos Aires, Argentina
- ³¹ California State University, Long Beach, CA, USA
- ³² Cavendish Laboratory, University of Cambridge, Cambridge, UK
- ³³ ^(a)Department of Physics, University of Cape Town, Cape Town, South Africa; ^(b)iThemba Labs, Western Cape, South Africa; ^(c)Department of Mechanical Engineering Science, University of Johannesburg, Johannesburg, South Africa; ^(d)Department of Physics, University of South Africa, Pretoria, South Africa; ^(e)School of Physics, University of the Witwatersrand, Johannesburg, South Africa
- ³⁴ Department of Physics, Carleton University, Ottawa, ON, Canada
- ³⁵ ^(a)Faculté des Sciences Ain Chock, Réseau Universitaire de Physique des Hautes Energies - Université Hassan II, Casablanca, Morocco; ^(b)Faculté des Sciences, Université Ibn-Tofail, Kénitra, Morocco; ^(c)Faculté des Sciences Semlalia, Université Cadi Ayyad, LPHEA, Marrakech, Morocco; ^(d)Moroccan Foundation for Advanced Science Innovation and Research (MAScIR), Rabat, Morocco; ^(e)LPMR, Faculté des Sciences, Université Mohamed Premier, Oujda, Morocco; ^(f)Faculté des sciences, Université Mohammed V, Rabat, Morocco
- ³⁶ CERN, Geneva, Switzerland
- ³⁷ Enrico Fermi Institute, University of Chicago, Chicago, IL, USA
- ³⁸ LPC, Université Clermont Auvergne, CNRS/IN2P3, Clermont-Ferrand, France
- ³⁹ Nevis Laboratory, Columbia University, Irvington, NY, USA
- ⁴⁰ Niels Bohr Institute, University of Copenhagen, Copenhagen, Denmark
- ⁴¹ ^(a)Dipartimento di Fisica, Università della Calabria, Rende, Italy; ^(b)INFN Gruppo Collegato di Cosenza, Laboratori Nazionali di Frascati, Frascati, Italy
- ⁴² Physics Department, Southern Methodist University, Dallas, TX, USA
- ⁴³ Physics Department, University of Texas at Dallas, Richardson, TX, USA
- ⁴⁴ National Centre for Scientific Research “Demokritos”, Agia Paraskevi, Greece
- ⁴⁵ ^(a)Department of Physics, Stockholm University, Stockholm, Sweden; ^(b)Oskar Klein Centre, Stockholm, Sweden
- ⁴⁶ Deutsches Elektronen-Synchrotron DESY, Hamburg and Zeuthen, Germany
- ⁴⁷ Lehrstuhl für Experimentelle Physik IV, Technische Universität Dortmund, Dortmund, Germany
- ⁴⁸ Institut für Kern- und Teilchenphysik, Technische Universität Dresden, Dresden, Germany
- ⁴⁹ Department of Physics, Duke University, Durham, NC, USA
- ⁵⁰ SUPA, School of Physics and Astronomy, University of Edinburgh, Edinburgh, UK
- ⁵¹ INFN e Laboratori Nazionali di Frascati, Frascati, Italy
- ⁵² Physikalisches Institut, Albert-Ludwigs-Universität Freiburg, Freiburg, Germany

- 53 II. Physikalisches Institut, Georg-August-Universität Göttingen, Göttingen, Germany
- 54 Département de Physique Nucléaire et Corpusculaire, Université de Genève, Geneva, Switzerland
- 55 (a)Dipartimento di Fisica, Università di Genova, Genoa, Italy; (b)INFN Sezione di Genova, Genoa, Italy
- 56 II. Physikalisches Institut, Justus-Liebig-Universität Giessen, Giessen, Germany
- 57 SUPA, School of Physics and Astronomy, University of Glasgow, Glasgow, UK
- 58 LPSC, Université Grenoble Alpes, CNRS/IN2P3, Grenoble INP, Grenoble, France
- 59 Laboratory for Particle Physics and Cosmology, Harvard University, Cambridge, MA, USA
- 60 (a)Department of Modern Physics and State Key Laboratory of Particle Detection and Electronics, University of Science and Technology of China, Hefei, China; (b)Institute of Frontier and Interdisciplinary Science and Key Laboratory of Particle Physics and Particle Irradiation (MOE), Shandong University, Qingdao, China; (c)School of Physics and Astronomy, Shanghai Jiao Tong University, Key Laboratory for Particle Astrophysics and Cosmology (MOE), SKLPPC, Shanghai, China; (d)Tsung-Dao Lee Institute, Shanghai, China
- 61 (a)Kirchhoff-Institut für Physik, Ruprecht-Karls-Universität Heidelberg, Heidelberg, Germany; (b)Physikalisches Institut, Ruprecht-Karls-Universität Heidelberg, Heidelberg, Germany
- 62 (a)Department of Physics, Chinese University of Hong Kong, Shatin N.T., Hong Kong; (b)Department of Physics, University of Hong Kong, Pok Fu Lam, Hong Kong; (c)Department of Physics and Institute for Advanced Study, Hong Kong University of Science and Technology, Clear Water Bay, Kowloon, Hong Kong
- 63 Department of Physics, National Tsing Hua University, Hsinchu, Taiwan
- 64 IJCLab, Université Paris-Saclay, CNRS/IN2P3, 91405 Orsay, France
- 65 Department of Physics, Indiana University, Bloomington, IN, USA
- 66 (a)INFN Gruppo Collegato di Udine, Sezione di Trieste, Udine, Italy; (b)ICTP, Trieste, Italy; (c)Dipartimento Politecnico di Ingegneria e Architettura, Università di Udine, Udine, Italy
- 67 (a)INFN Sezione di Lecce, Lecce, Italy; (b)Dipartimento di Matematica e Fisica, Università del Salento, Lecce, Italy
- 68 (a)INFN Sezione di Milano, Milan, Italy; (b)Dipartimento di Fisica, Università di Milano, Milan, Italy
- 69 (a)INFN Sezione di Napoli, Naples, Italy; (b)Dipartimento di Fisica, Università di Napoli, Naples, Italy
- 70 (a)INFN Sezione di Pavia, Pavia, Italy; (b)Dipartimento di Fisica, Università di Pavia, Pavia, Italy
- 71 (a)INFN Sezione di Pisa, Pisa, Italy; (b)Dipartimento di Fisica E. Fermi, Università di Pisa, Pisa, Italy
- 72 (a)INFN Sezione di Roma, Rome, Italy; (b)Dipartimento di Fisica, Sapienza Università di Roma, Rome, Italy
- 73 (a)INFN Sezione di Roma Tor Vergata, Rome, Italy; (b)Dipartimento di Fisica, Università di Roma Tor Vergata, Rome, Italy
- 74 (a)INFN Sezione di Roma Tre, Rome, Italy; (b)Dipartimento di Matematica e Fisica, Università Roma Tre, Rome, Italy
- 75 (a)INFN-TIFPA, Povo, Italy; (b)Università degli Studi di Trento, Trento, Italy
- 76 Institut für Astro- und Teilchenphysik, Leopold-Franzens-Universität, Innsbruck, Austria
- 77 University of Iowa, Iowa City, IA, USA
- 78 Department of Physics and Astronomy, Iowa State University, Ames, IA, USA
- 79 Joint Institute for Nuclear Research, Dubna, Russia
- 80 (a)Departamento de Engenharia Elétrica, Universidade Federal de Juiz de Fora (UFJF), Juiz de Fora, Brazil; (b)Universidade Federal do Rio De Janeiro COPPE/EE/IF, Rio de Janeiro, Brazil; (c)Instituto de Física, Universidade de São Paulo, São Paulo, Brazil
- 81 KEK, High Energy Accelerator Research Organization, Tsukuba, Japan
- 82 Graduate School of Science, Kobe University, Kobe, Japan
- 83 (a)AGH University of Science and Technology, Faculty of Physics and Applied Computer Science, Kraków, Poland; (b)Marian Smoluchowski Institute of Physics, Jagiellonian University, Kraków, Poland
- 84 Institute of Nuclear Physics Polish Academy of Sciences, Kraków, Poland
- 85 Faculty of Science, Kyoto University, Kyoto, Japan
- 86 Kyoto University of Education, Kyoto, Japan
- 87 Research Center for Advanced Particle Physics and Department of Physics, Kyushu University, Fukuoka, Japan
- 88 Instituto de Física La Plata, Universidad Nacional de La Plata and CONICET, La Plata, Argentina
- 89 Physics Department, Lancaster University, Lancaster, UK
- 90 Oliver Lodge Laboratory, University of Liverpool, Liverpool, UK
- 91 Department of Experimental Particle Physics, Jožef Stefan Institute and Department of Physics, University of Ljubljana, Ljubljana, Slovenia
- 92 School of Physics and Astronomy, Queen Mary University of London, London, UK

- ⁹³ Department of Physics, Royal Holloway University of London, Egham, UK
- ⁹⁴ Department of Physics and Astronomy, University College London, London, UK
- ⁹⁵ Louisiana Tech University, Ruston, LA, USA
- ⁹⁶ Fysiska institutionen, Lunds universitet, Lund, Sweden
- ⁹⁷ Centre de Calcul de l'Institut National de Physique Nucléaire et de Physique des Particules (IN2P3), Villeurbanne, France
- ⁹⁸ Departamento de Física Teórica C-15 and CIAFF, Universidad Autónoma de Madrid, Madrid, Spain
- ⁹⁹ Institut für Physik, Universität Mainz, Mainz, Germany
- ¹⁰⁰ School of Physics and Astronomy, University of Manchester, Manchester, UK
- ¹⁰¹ CPPM, Aix-Marseille Université, CNRS/IN2P3, Marseille, France
- ¹⁰² Department of Physics, University of Massachusetts, Amherst, MA, USA
- ¹⁰³ Department of Physics, McGill University, Montreal, QC, Canada
- ¹⁰⁴ School of Physics, University of Melbourne, Melbourne, VIC, Australia
- ¹⁰⁵ Department of Physics, University of Michigan, Ann Arbor, MI, USA
- ¹⁰⁶ Department of Physics and Astronomy, Michigan State University, East Lansing, MI, USA
- ¹⁰⁷ B.I. Stepanov Institute of Physics, National Academy of Sciences of Belarus, Minsk, Belarus
- ¹⁰⁸ Research Institute for Nuclear Problems of Byelorussian State University, Minsk, Belarus
- ¹⁰⁹ Group of Particle Physics, University of Montreal, Montreal, QC, Canada
- ¹¹⁰ P.N. Lebedev Physical Institute of the Russian Academy of Sciences, Moscow, Russia
- ¹¹¹ National Research Nuclear University MEPhI, Moscow, Russia
- ¹¹² D.V. Skobeltsyn Institute of Nuclear Physics, M.V. Lomonosov Moscow State University, Moscow, Russia
- ¹¹³ Fakultät für Physik, Ludwig-Maximilians-Universität München, Munich, Germany
- ¹¹⁴ Max-Planck-Institut für Physik (Werner-Heisenberg-Institut), Munich, Germany
- ¹¹⁵ Nagasaki Institute of Applied Science, Nagasaki, Japan
- ¹¹⁶ Graduate School of Science and Kobayashi-Maskawa Institute, Nagoya University, Nagoya, Japan
- ¹¹⁷ Department of Physics and Astronomy, University of New Mexico, Albuquerque, NM, USA
- ¹¹⁸ Institute for Mathematics, Astrophysics and Particle Physics, Radboud University/Nikhef, Nijmegen, The Netherlands
- ¹¹⁹ Nikhef National Institute for Subatomic Physics and University of Amsterdam, Amsterdam, The Netherlands
- ¹²⁰ Department of Physics, Northern Illinois University, DeKalb, IL, USA
- ¹²¹ ^(a)Budker Institute of Nuclear Physics and NSU, SB RAS, Novosibirsk, Russia; ^(b)Novosibirsk State University, Novosibirsk, Russia
- ¹²² Institute for High Energy Physics of the National Research Centre Kurchatov Institute, Protvino, Russia
- ¹²³ Institute for Theoretical and Experimental Physics named by A.I. Alikhanov of National Research Centre “Kurchatov Institute”, Moscow, Russia
- ¹²⁴ Department of Physics, New York University, New York, NY, USA
- ¹²⁵ Ochanomizu University, Otsuka, Bunkyo-ku, Tokyo, Japan
- ¹²⁶ Ohio State University, Columbus, OH, USA
- ¹²⁷ Homer L. Dodge Department of Physics and Astronomy, University of Oklahoma, Norman, OK, USA
- ¹²⁸ Department of Physics, Oklahoma State University, Stillwater, OK, USA
- ¹²⁹ Palacký University, RCPTM, Joint Laboratory of Optics, Olomouc, Czech Republic
- ¹³⁰ Institute for Fundamental Science, University of Oregon, Eugene, OR, USA
- ¹³¹ Graduate School of Science, Osaka University, Osaka, Japan
- ¹³² Department of Physics, University of Oslo, Oslo, Norway
- ¹³³ Department of Physics, Oxford University, Oxford, UK
- ¹³⁴ LPNHE, Sorbonne Université, Université de Paris, CNRS/IN2P3, Paris, France
- ¹³⁵ Department of Physics, University of Pennsylvania, Philadelphia, PA, USA
- ¹³⁶ Konstantinov Nuclear Physics Institute of National Research Centre “Kurchatov Institute”, PNPI, St. Petersburg, Russia
- ¹³⁷ Department of Physics and Astronomy, University of Pittsburgh, Pittsburgh, PA, USA
- ¹³⁸ ^(a)Laboratório de Instrumentação e Física Experimental de Partículas, LIP, Lisbon, Portugal; ^(b)Departamento de Física, Faculdade de Ciências, Universidade de Lisboa, Lisbon, Portugal; ^(c)Departamento de Física, Universidade de Coimbra, Coimbra, Portugal; ^(d)Centro de Física Nuclear da Universidade de Lisboa, Lisbon, Portugal; ^(e)Departamento de Física, Universidade do Minho, Braga, Portugal; ^(f)Departamento de Física Teórica y del Cosmos, Universidad de Granada,

- Granada, Spain; ^(g)Dep Física and CEFITEC of Faculdade de Ciências e Tecnologia, Universidade Nova de Lisboa, Caparica, Portugal; ^(h)Instituto Superior Técnico, Universidade de Lisboa, Lisbon, Portugal
- 139 Institute of Physics of the Czech Academy of Sciences, Prague, Czech Republic
- 140 Czech Technical University in Prague, Prague, Czech Republic
- 141 Faculty of Mathematics and Physics, Charles University, Prague, Czech Republic
- 142 Particle Physics Department, Rutherford Appleton Laboratory, Didcot, UK
- 143 IRFU, CEA, Université Paris-Saclay, Gif-sur-Yvette, France
- 144 Santa Cruz Institute for Particle Physics, University of California Santa Cruz, Santa Cruz, CA, USA
- 145 ^(a)Departamento de Física, Pontificia Universidad Católica de Chile, Santiago, Chile; ^(b)Universidad Andres Bello, Department of Physics, Santiago, Chile; ^(c)Instituto de Alta Investigación, Universidad de Tarapacá, Santiago, Chile; ^(d)Departamento de Física, Universidad Técnica Federico Santa María, Valparaíso, Chile
- 146 Universidade Federal de São João del Rei (UFSJ), São João del Rei, Brazil
- 147 Department of Physics, University of Washington, Seattle, WA, USA
- 148 Department of Physics and Astronomy, University of Sheffield, Sheffield, UK
- 149 Department of Physics, Shinshu University, Nagano, Japan
- 150 Department Physik, Universität Siegen, Siegen, Germany
- 151 Department of Physics, Simon Fraser University, Burnaby, BC, Canada
- 152 SLAC National Accelerator Laboratory, Stanford, CA, USA
- 153 Physics Department, Royal Institute of Technology, Stockholm, Sweden
- 154 Departments of Physics and Astronomy, Stony Brook University, Stony Brook, NY, USA
- 155 Department of Physics and Astronomy, University of Sussex, Brighton, UK
- 156 School of Physics, University of Sydney, Sydney, Australia
- 157 Institute of Physics, Academia Sinica, Taipei, Taiwan
- 158 ^(a)E. Andronikashvili Institute of Physics, Iv. Javakhishvili Tbilisi State University, Tbilisi, Georgia; ^(b)High Energy Physics Institute, Tbilisi State University, Tbilisi, Georgia
- 159 Department of Physics, Technion, Israel Institute of Technology, Haifa, Israel
- 160 Raymond and Beverly Sackler School of Physics and Astronomy, Tel Aviv University, Tel Aviv, Israel
- 161 Department of Physics, Aristotle University of Thessaloniki, Thessaloniki, Greece
- 162 International Center for Elementary Particle Physics and Department of Physics, University of Tokyo, Tokyo, Japan
- 163 Department of Physics, Tokyo Institute of Technology, Tokyo, Japan
- 164 Tomsk State University, Tomsk, Russia
- 165 Department of Physics, University of Toronto, Toronto, ON, Canada
- 166 ^(a)TRIUMF, Vancouver, BC, Canada; ^(b)Department of Physics and Astronomy, York University, Toronto, ON, Canada
- 167 Division of Physics and Tomonaga Center for the History of the Universe, Faculty of Pure and Applied Sciences, University of Tsukuba, Tsukuba, Japan
- 168 Department of Physics and Astronomy, Tufts University, Medford, MA, USA
- 169 Department of Physics and Astronomy, University of California Irvine, Irvine, CA, USA
- 170 Department of Physics and Astronomy, University of Uppsala, Uppsala, Sweden
- 171 Department of Physics, University of Illinois, Urbana, IL, USA
- 172 Instituto de Física Corpuscular (IFIC), Centro Mixto Universidad de Valencia - CSIC, Valencia, Spain
- 173 Department of Physics, University of British Columbia, Vancouver, BC, Canada
- 174 Department of Physics and Astronomy, University of Victoria, Victoria, BC, Canada
- 175 Fakultät für Physik und Astronomie, Julius-Maximilians-Universität Würzburg, Würzburg, Germany
- 176 Department of Physics, University of Warwick, Coventry, UK
- 177 Waseda University, Tokyo, Japan
- 178 Department of Particle Physics and Astrophysics, Weizmann Institute of Science, Rehovot, Israel
- 179 Department of Physics, University of Wisconsin, Madison, WI, USA
- 180 Fakultät für Mathematik und Naturwissenschaften, Fachgruppe Physik, Bergische Universität Wuppertal, Wuppertal, Germany
- 181 Department of Physics, Yale University, New Haven, CT, USA

^a Also at: Borough of Manhattan Community College, City University of New York, New York, NY, USA

^b Also at: Bruno Kessler Foundation, Trento, Italy

- ^c Also at: Center for High Energy Physics, Peking University, Beijing, China
- ^d Also at: Centro Studi e Ricerche Enrico Fermi, Rome, Italy
- ^e Also at: CERN, Geneva, Switzerland
- ^f Also at: CPPM, Aix-Marseille Université, CNRS/IN2P3, Marseille, France
- ^g Also at: Département de Physique Nucléaire et Corpusculaire, Université de Genève, Geneva, Switzerland
- ^h Also at: Departament de Física de la Universitat Autònoma de Barcelona, Barcelona, Spain
- ⁱ Also at: Department of Financial and Management Engineering, University of the Aegean, Chios, Greece
- ^j Also at: Department of Physics and Astronomy, Michigan State University, East Lansing, MI, USA
- ^k Also at: Department of Physics and Astronomy, University of Louisville, Louisville, KY, USA
- ^l Also at: Department of Physics, Ben Gurion University of the Negev, Beer Sheva, Israel
- ^m Also at: Department of Physics, California State University, East Bay, USA
- ⁿ Also at: Department of Physics, California State University, Fresno, USA
- ^o Also at: Department of Physics, California State University, Sacramento, USA
- ^p Also at: Department of Physics, King's College London, London, UK
- ^q Also at: Department of Physics, St. Petersburg State Polytechnical University, St. Petersburg, Russia
- ^r Also at: Department of Physics, University of Fribourg, Fribourg, Switzerland
- ^s Also at: Faculty of Physics, M.V. Lomonosov Moscow State University, Moscow, Russia
- ^t Also at: Faculty of Physics, Sofia University, 'St. Kliment Ohridski', Sofia, Bulgaria
- ^u Also at: Giresun University, Faculty of Engineering, Giresun, Turkey
- ^v Also at: Graduate School of Science, Osaka University, Osaka, Japan
- ^w Also at: Hellenic Open University, Patras, Greece
- ^x Also at: Institutio Catalana de Recerca i Estudis Avancats, ICREA, Barcelona, Spain
- ^y Also at: Institut für Experimentalphysik, Universität Hamburg, Hamburg, Germany
- ^z Also at: Institute for Nuclear Research and Nuclear Energy (INRNE) of the Bulgarian Academy of Sciences, Sofia, Bulgaria
- ^{aa} Also at: Institute for Particle and Nuclear Physics, Wigner Research Centre for Physics, Budapest, Hungary
- ^{ab} Also at: Institute of Particle Physics (IPP), Toronto, Canada
- ^{ac} Also at: Institute of Physics, Azerbaijan Academy of Sciences, Baku, Azerbaijan
- ^{ad} Also at: Instituto de Física Teórica, IFT-UAM/CSIC, Madrid, Spain
- ^{ae} Also at: Department of Physics, Istanbul University, Istanbul, Turkey
- ^{af} Also at: Joint Institute for Nuclear Research, Dubna, Russia
- ^{ag} Also at: Moscow Institute of Physics and Technology State University, Dolgoprudny, Russia
- ^{ah} Also at: National Research Nuclear University MEPhI, Moscow, Russia
- ^{ai} Also at: Physics Department, An-Najah National University, Nablus, Palestine
- ^{aj} Also at: Physikalisches Institut, Albert-Ludwigs-Universität Freiburg, Freiburg, Germany
- ^{ak} Also at: The City College of New York, New York, NY, USA
- ^{al} Also at: TRIUMF, Vancouver, BC, Canada
- ^{am} Also at: Università di Napoli Parthenope, Naples, Italy
- ^{an} Also at: University of Chinese Academy of Sciences (UCAS), Beijing, China
- * Deceased